

# Lombardi Drawings of Knots and Links

Philipp Kindermann<sup>1</sup>, Stephen Kobourov<sup>2</sup>, Maarten Löffler<sup>3</sup>,  
Martin Nöllenburg<sup>4</sup>, André Schulz<sup>1</sup>, and Birgit Vogtenhuber<sup>6</sup>

<sup>1</sup> FernUniversität in Hagen, Germany, `firstname.lastname@fernuni-hagen.de`

<sup>2</sup> University of Arizona, Tucson, AZ, US, `kobourov@cs.arizona.edu`

<sup>3</sup> Universiteit Utrecht, The Netherlands, `m.loffler@uu.nl`

<sup>4</sup> TU Wien, Vienna, Austria, `noellenburg@ac.tuwien.ac.at`

<sup>5</sup> Graz University of Technology, Austria, `bvogt@ist.tugraz.at`

**Abstract.** Knot and link diagrams are projections of one or more 3-dimensional simple closed curves into  $\mathbb{R}^2$ , such that no more than two points project to the same point in  $\mathbb{R}^2$ . These diagrams are drawings of 4-regular plane multigraphs. Knots are typically smooth curves in  $\mathbb{R}^3$ , so their projections should be smooth curves in  $\mathbb{R}^2$  with good continuity and large crossing angles: exactly the properties of Lombardi graph drawings (defined by circular-arc edges and perfect angular resolution).

We show that several knots do not allow Lombardi drawings. On the other hand, we identify a large class of 4-regular plane multigraphs that do have Lombardi drawings. We then study two relaxations of Lombardi drawings and show that every knot admits a plane 2-Lombardi drawing (where edges are composed of two circular arcs). Further, every knot is *near-Lombardi*, that is, it can be drawn as Lombardi drawing when relaxing the angular resolution requirement by an arbitrary small angular offset  $\varepsilon$ , while maintaining a  $180^\circ$  angle between opposite edges.



Fig. 1: Hand-made drawings of knots from the books of Rolfsen [14] (left), Livingston [13] (middle), and Kauffman [11] (right).

## 1 Introduction

A *knot* is an embedding of a simple closed curve in 3-dimensional Euclidean space  $\mathbb{R}^3$ . Similarly, a *link* is a collection of simple closed curves in  $\mathbb{R}^3$ . A *drawing of a knot (link)* (also known as *knot diagram*) is a projection of the knot (link) to the Euclidean plane  $\mathbb{R}^2$  such that for any point of  $\mathbb{R}^2$ , at most two points of the curve(s) are mapped to it [6, 14, 15]. From a graph drawing perspective, drawings of knots and links are drawings of 4-regular plane multigraphs that

contain neither loops nor cut vertices. Likewise, every 4-regular plane multigraph without loops and cut vertices can be interpreted as a link. Unless specified otherwise, we assume that a multigraph has no self-loops or cut vertices.

In this paper, we address a question that was recently posed by Benjamin  
 5 Burton: “Given a drawing of a knot, how can it be redrawn *nicely* without  
 changing the given topology of the drawing?” We do know what a drawing of  
 a knot is, but what is meant by a *nice* drawing? Several graphical annotations  
 of knots and links as graphs have been proposed in the knot theory literature,  
 but most of the illustrations are hand-drawn; see Fig. 1. When studying these  
 10 drawings, a few desirable features become apparent: (i) edges are typically drawn  
 as smooth curves, (ii) the angular resolution of the underlying 4-regular graph  
 is close to  $90^\circ$ , and (iii) the drawing preserves the continuity of the knot, that is,  
 in every vertex of the underlying graph, opposite edges have a common tangent.

There already exists a graph drawing style that fulfills the requirements  
 15 above: a *Lombardi drawing* of a (multi-)graph  $G = (V, E)$  is a drawing of  $G$   
 in the Euclidean plane with the following properties:

1. The vertices are represented as distinct points in the plane
2. The edges are represented as circular arcs connecting the representations of  
 their end vertices (and not containing the representation of any other vertex);  
 20 note that a straight-line segment is a circular arc with radius infinity.
3. Every vertex has *perfect angular resolution*, i.e., its incident edges are equi-  
 angularly spaced. For knots and links this means that the angle between any  
 two consecutive edges is  $90^\circ$ .

A Lombardi drawing is plane if none of its edges intersect. Note that we are  
 25 particularly interested in plane Lombardi drawings, since crossings change the  
 topology of the drawn knot.

*Knot drawing software:* Software for generating drawings for knots and links ex-  
 ists. One powerful package is `KnotPlot` [15], which provides several methods for  
 drawing knot diagrams. It contains a library of over 1,000 precomputed knots  
 30 and can also generate knot drawings of certain families, such as torus knots.  
`KnotPlot` also provides methods for drawing general knots based on the of the  
 underlying plane multigraph. By replacing every vertex by a 4-cycle, the multi-  
 graph becomes a simple planar 3-connected graph, which is then using Tutte’s  
 barycentric method [17]. In the end, the modifications are reversed and a dra-  
 35 wing of the knot is obtained with edges drawn as polygonal arcs. The author  
 noticed that this method “... does not yield ‘pleasing’ graphs or knot diagrams.”  
 In particular, he noticed issues with vertex and angular resolution [15, pg. 102].  
 Another approach was used by Emily Redelmeier [1]. Here, every arc, crossing,  
 and face of the knot diagram is associated with a disk. The drawing is then  
 40 generated from the implied circle packing as a circular arc drawing. As a result  
 of the construction, every edge in the diagram is made of three circular arcs with  
 common tangents at opposite edges. Since no further details are given, it is hard  
 to evaluate the effectiveness of this approach, although as we show in this paper,  
 three circular arcs per edge are never needed.

*Lombardi drawings:* Lombardi drawings were introduced by Duncan et al. [8]. They showed that 2-degenerate graphs have Lombardi drawings and that all  $d$ -regular graphs, with  $d \not\equiv 2 \pmod{4}$ , have Lombardi drawings with all vertices placed along a common circle. Neither of these results, however, is guaranteed to result in plane drawings. Duncan et al. [8] also shows that there exist planar graphs that do not have plane Lombardi drawings, but restricted graph classes (e.g., Halin graphs) do. In subsequent work, Eppstein [9,10] showed that every (simple) planar graph with maximum degree three has a plane Lombardi drawing. Further, he showed that a certain class of 4-regular planar graphs (the medial graphs of polyhedral graphs) also admit plane Lombardi drawings and he presented an example of a 4-regular planar graph that does not have a plane Lombardi drawing. A generalization of Lombardi drawings are  $k$ -Lombardi drawings. Here, every edge is a sequence of at most  $k$  circular arcs that meet at a common tangent. Duncan et al. [7] showed that every planar graph has a plane 3-Lombardi drawing. Related to  $k$ -Lombardi-drawings are *smooth-orthogonal drawings of complexity  $k$*  [4]. These are plane drawings where every edge consists of a sequence of at most  $k$  quarter-circles and axis-aligned segments that meet smoothly, edges are axis-aligned (emanate from a vertex either horizontally or vertically), and no two edges emanate in the same direction. Note that in the special case of 4-regular graphs, smooth-orthogonal drawings of complexity  $k$  are also plane  $k$ -Lombardi drawings.

*Our Contributions:* The main question we study here is motivated by the application of the Lombardi drawing style to knot and link drawings: Given a 4-regular plane multigraph  $G$  without loops and cut vertices, does  $G$  admit a plane Lombardi drawing with the same combinatorial embedding? In Sect. 2 we start with some positive results on extending a plane Lombardi drawing, as well as composing two plane Lombardi drawings. In Sect. 3, by extending the results of Eppstein [9,10], we show that a large class of multigraphs, including 4-regular polyhedral graphs, does have plane Lombardi drawings. Unfortunately, there exist several small knots that do not have a plane Lombardi drawing. Section 4 discusses these cases but also lists a few positive results for small examples. In Sect. 5, we show that every 4-regular plane multigraph has a plane 2-Lombardi drawing. In Sect. 6, we show that every 4-regular plane multigraph can be drawn with non-crossing circular arcs, so that the perfect angular resolution criterion is violated only by an arbitrarily small value  $\varepsilon$ , while maintaining that opposite edges have common tangents.

## 2 General Observations

If a knot or a link has a plane Lombardi drawing, we call it a *plane Lombardi knot (link)*. We further call the property of admitting a plane Lombardi drawing *plane Lombardiness*. If two vertices in a plane Lombardi drawing of a knot are connected by a pair of multi-edges, we denote the face enclosed by these two edges as a *lens*.

*Property 1 (Property 2 in [7, 8]).* Let  $u$  and  $v$  be two vertices with given positions that have a common, unplaced neighbor  $w$ . Let  $d_u$  and  $d_v$  be two tangent directions and let  $\theta$  be a target angle. Let  $C$  be the locus of all positions for placing  $w$  so that (i) the edge  $(u, w)$  is a circular arc leaving  $u$  in direction  $d_u$ ,  
 5 (ii) the edge  $(v, w)$  is a circular arc leaving  $v$  in direction  $d_v$ , and (iii) the angle formed at  $w$  is  $\theta$ . Then  $C$  is a circle, the so-called *placement circle* of  $w$ .

Duncan et al. [7] further specify the radius and center of the placement circle by the input coordinates and angles. For the special case that the two tangent directions  $d_u$  and  $d_v$  are symmetric with respect to the line through  $u$  and  $v$ ,  
 10 and that the angle  $\theta$  is  $90^\circ$  or  $270^\circ$ , the corresponding placement circle is such that its tangent lines at  $u$  and  $v$  form an angle of  $45^\circ$  with the arc directions  $d_u$  and  $d_v$ . In particular, the placement circle bisects the right angle between  $d_u$  (resp.  $d_v$ ) and its neighboring arc direction. Fig. 2 illustrates this situation.

There exist a number of operations that maintain the plane Lombardiness of  
 15 a 4-regular multigraph. Two knots  $A$  and  $B$  can be combined by cutting them open and gluing twice a pair of loose ends from  $A$  and  $B$ . This operation is known as a *knot sum*  $A + B$ . Knots that cannot be decomposed into a sum of two smaller knots are known as *prime knots*. By Schubert's theorem, every knot can be uniquely decomposed into prime knots [16]. The smallest prime knot is  
 20 the trefoil knot with three crossings or vertices; see Fig. 1(right). Rolfsen's knot table<sup>1</sup> lists all prime knots with up to ten vertices. The Alexander-Briggs-Rolfsen notation [3, 14] is a well established notation that organizes these knots by their vertex number and a counting index, e.g., the trefoil knot  $3_1$  is listed as the first (and only) knot with three vertices.

**Theorem 1.** *Let  $A$  and  $B$  be two 4-regular multigraphs with plane Lombardi drawings. Let  $a$  be an edge of  $A$  and  $b$  an edge of  $B$ . Then the knot sum  $A + B$ , obtained by connecting  $A$  and  $B$  along edges  $a$  and  $b$ , admits a plane Lombardi drawing.*  
 25

*Sketch of Proof.* The idea of the composition is sketched in Fig. 3. We first apply  
 30 Möbius transformations, rotations, and translations to the two drawings so that edges  $a$  and  $b$  can be aligned along a circle with infinite radius. This can be done such that the drawings of  $A$  and  $B$  do not intersect after removing  $a$  and  $b$ . We can now reconnect the two drawings into a single plane Lombardi drawing by introducing two edges  $c$  and  $d$  along the straight line.  $\square$

Another operation that preserves the plane Lombardiness is *lens multiplication*.  
 35 Let  $G = (V, E)$  be a 4-regular plane multigraph with a lens between two vertices  $u$  and  $v$ . A lens multiplication of  $G$  is a 4-regular plane multigraph that is obtained by replacing the lens between  $u$  and  $v$  with a chain of lenses.

**Lemma 1.** *Let  $G = (V, E)$  be a 4-regular plane multigraph with a plane Lombardi drawing  $\Gamma$ . Then, any lens multiplication  $G'$  of  $G$  also admits a plane Lombardi drawing.*  
 40

<sup>1</sup> [http://katlas.org/wiki/The\\_Rolfsen\\_Knot\\_Table](http://katlas.org/wiki/The_Rolfsen_Knot_Table)

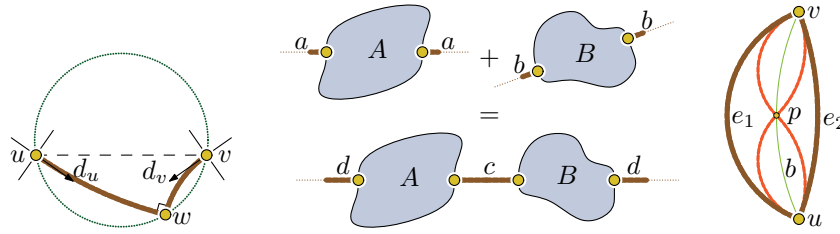


Fig. 2: Placement circle for neighbor  $w$  of  $u$  and  $v$  in a 4-regular graph. Fig. 3: Adding two plane Lombardi drawings of 4-regular multigraphs. Fig. 4: Subdividing a lens between  $u$  and  $v$  by a new vertex  $p$ .

*Sketch of Proof.* Let  $f$  be a lens in  $\Gamma$  spanned by two vertices  $u$  and  $v$  as shown in Fig. 4. We draw a bisecting circular arc  $b$  that splits the angles at  $u$  and  $v$  into two  $45^\circ$  angles. Now we can draw any chain of lenses inside  $f$  by placing the additional vertices on  $b$ . The resulting drawing is a plane Lombardi drawing.  $\square$

### 3 Plane Lombardi Drawings via Circle Packing

Recall that *polyhedral graphs* are simple planar 3-connected graphs, and that those graphs have a unique (plane) combinatorial embedding. The (plane) *dual graph*  $M'$  of a plane graph  $M$  has a vertex for every face of  $M$  and an edge between two vertices for every edge shared by the corresponding faces in  $M$ . In the “classic” drawing  $D(M, M')$  of a primal-dual graph pair  $(M, M')$ , every vertex of  $M'$  lies in its corresponding face of  $M$  and vice versa, and every edge of  $M'$  intersects exactly its corresponding edge of  $M$ . Hence, every cell of  $D(M, M')$  has exactly two such edge crossings and exactly one vertex of each of  $M$  and  $M'$  on its boundary. The *medial graph* of a primal-dual graph pair  $(M, M')$  has a vertex for every crossing edge pair in  $D(M, M')$  and an edge between two vertices whenever they share a cell in  $D(M, M')$ ; see Fig. 5a. Every cell of the medial graph contains either a vertex of  $M$  or a vertex of  $M'$  and every edge in the medial graph is incident to exactly one cell in  $D(M, M')$ .

Every 4-regular plane multigraph  $G$  can be interpreted as the medial graph of some plane graph  $M$  and its dual  $M'$ , where both graphs possibly contain multi-edges. If  $G$  contains no loops and cut vertices, then neither  $M$  nor  $M'$  contains loops. Eppstein [9] showed that if  $M$  (and hence also  $M'$ ) is polyhedral, then  $G$  admits a plane Lombardi drawing. We show next how to extend this result to a larger graph class. We only give a short sketch of the proof here. The full proof, as well as an example of the algorithm is in Appendix B.

**Theorem 2.** *Let  $G = (V, E)$  be a biconnected 4-regular plane multigraph and let  $M$  and  $M'$  be the primal-dual multigraph pair for which  $G$  is the medial graph. If one of  $M$  and  $M'$  is simple, then  $G$  admits a plane Lombardi drawing preserving its embedding.*

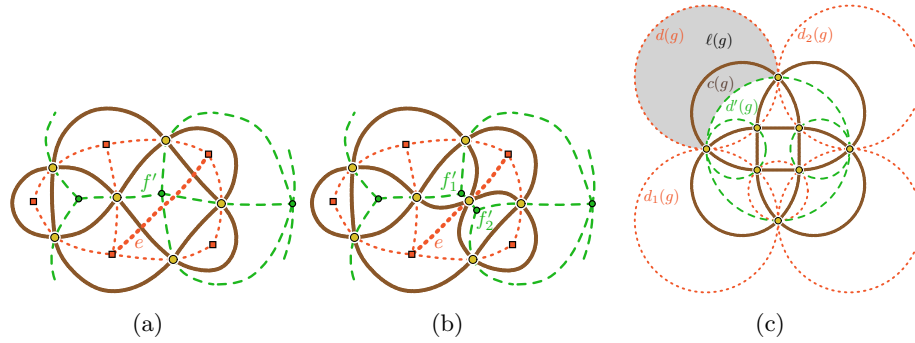


Fig. 5: (a)–(b) Modifications due to an edge addition and (c) a primal-dual circle packing. The medial graph  $G$  is drawn solid, the primal  $M$  is drawn dotted, and the dual  $M'$  is drawn dashed. The shaded area is the lens region  $\ell(g)$ .

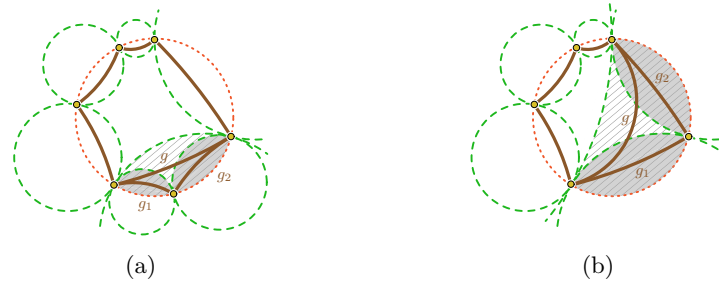


Fig. 6: Two examples of a lens region  $\ell(g)$  resulting from  $\ell(g_1)$  and  $\ell(g_2)$ : (a) convex and (b) reflex. The lens regions of  $g_1$  and  $g_2$  are drawn as shaded areas, while the one of  $g$  is the cross-hatched region.

*Sketch of Proof.* Assume w.l.o.g. that  $M$  is simple. If  $M$  (and hence also  $M'$ ) is polyhedral, then  $G$  admits a plane Lombardi drawing  $\Gamma$  by Eppstein [9]. Moreover,  $\Gamma$  is embedding-preserving (up to Möbius transformation), as the combinatorial embedding of  $M$  is unique (up to homeomorphism on the sphere).

5 If  $M$  is not 3-connected, we proceed in three steps. First, we augment  $M$  to a polyhedral graph  $M_p$  by iteratively adding  $p$  edges (any added edge splits a face of size at least four into two faces of size at least three). During this process, we also iteratively modify the dual graph and the medial graph as shown in Fig. 5a–b.

10 Second, we apply Eppstein’s result to obtain a primal-dual circle packing of  $M_p$  and  $M'_p$ , together with a Lombardi drawing  $\Gamma_p$  of the medial graph  $G_p$ ; see Fig. 5c. Finally, we revert the augmentation process from the first step by iteratively changing the plane Lombardi drawing  $\Gamma_p$  of  $G_p$  to a plane Lombardi drawing  $\Gamma$  of  $G$ . A main ingredient for this last step is the following: In the  
 15 primal-dual circle packing of  $M_p$  and  $M'_p$ , every edge  $g$  of  $\Gamma_p$  lies in a region  $\ell(g)$  that is bounded by a primal and a dual circle. This region  $\ell(g)$  is interior-disjoint

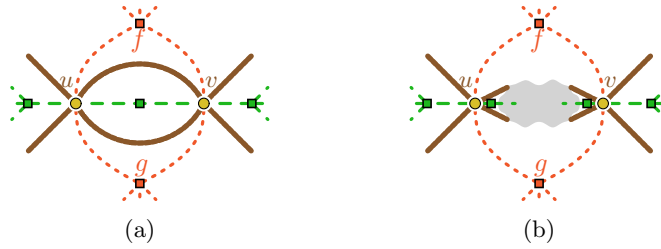


Fig. 7: If there is a multi-edge between vertices  $f$  and  $g$  in the primal, then there is a multi-edge  $(u, v)$  or a separation pair  $u, v$  in the medial.

with the region  $\ell(g')$  of any other edge  $g'$  of  $\Gamma_p$ . When removing an edge from the primal graph, a vertex is removed from the Lombardi drawing and the four incident edges are replaced by two edges connecting the non-common endpoints of the four edges. We show how to draw each new edge  $g$  that replaces  $g_1$  and  $g_2$  in a way that again has a uniquely assigned region  $\ell(g)$  that is interior-disjoint with the regions of all other edges; see Fig. 6 for a sketch.  $\square$

We remark that this result is not tight: there exist 4-regular plane multi-graphs whose primal-dual pair  $M$  and  $M'$  contain parallel edges that still admit plane Lombardi drawings, e.g., knots  $8_{12}$ ,  $8_{14}$ ,  $8_{15}$ ,  $8_{16}$ ; see Fig. 17 in Appendix C.

We now prove that 4-regular polyhedral graphs are medial graphs of a simple primal-dual pair.

**Lemma 2.** *Let  $G = (V, E)$  be a 4-regular polyhedral graph and let  $M$  and  $M'$  be the primal-dual pair for which  $G$  is the medial graph. If there is a multi-edge in  $M$  or in  $M'$ , then the corresponding vertices of  $G$  either have a multi-edge between them or they form a separation pair of  $G$ .*

*Proof.* W.l.o.g., assume that there are two edges between vertices  $f$  and  $g$  in  $M$ . Let  $u$  and  $v$  be the vertices of  $G$  that these two edges pass through; see Fig. 7. The vertices  $f$  and  $g$  of  $M$  correspond to faces in the embedding of  $G$  that both contain  $u$  and  $v$ . Hence, the removal of  $u$  and  $v$  from  $G$  disconnects  $G$  into two parts: the part inside the area spanned by the two edges between  $f$  and  $g$  and the part outside this area. Both  $u$  and  $v$  have two edges in both areas, so either there is a multi-edge between  $u$  and  $v$ , or there are vertices in both parts, which makes  $u, v$  a separation pair of  $G$ .  $\square$

Lemma 2 and Theorem 2 immediately give the following theorem.

**Theorem 3.** *Let  $G = (V, E)$  be a 4-regular polyhedral graph. Then  $G$  admits a plane Lombardi drawing.*

## 4 Positive and Negative Results for Small Graphs

We next consider all prime knots with 8 vertices or less. We compute plane Lombardi drawings for those that have it and argue that such drawings do not

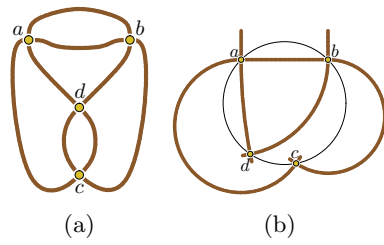


Fig. 8: Knot  $4_1$  (left) has no Lombardi drawing.

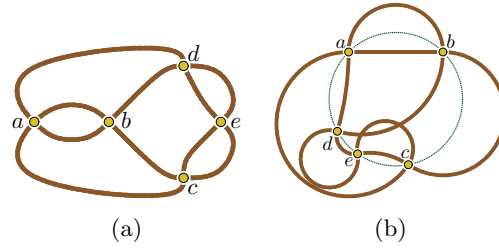


Fig. 9: Knot  $5_2$  and a non-plane Lombardi drawing.

exists for the others. We start by showing that no knot with a  $K_4$  subgraph is plane Lombardi.

**Lemma 3.** *Every 4-regular plane multigraph  $G$  that contains  $K_4$  as a subgraph does not admit a plane Lombardi drawing.*

5 *Proof.* Let  $a, b, c, d$  be the vertices of the  $K_4$ . Every plane embedding of  $K_4$  has a vertex that lies inside the cycle through the other 3 vertices; let  $d$  be this vertex. Since  $d$  has degree 4, it has another edge to either one of  $a, b, c$ , or to a different vertex. In the former case, assume that there is a multi-edge between  $c$  and  $d$ . In the latter case, by 4-regularity, there has to be another vertex of  $a, b, c$  that  
 10 is connected to a vertex inside the cycle through  $a, b, c$ ; let  $c$  be this vertex. In both cases,  $c$  has two edges that lie inside the cycle through  $a, b, c$ .

Assume that  $G$  has a Lombardi drawing. Since Möbius transformations do not change the properties of a Lombardi drawing, we may assume that the edge  $(a, b)$  is drawn as a straight-line segment as in Fig. 8b. Since both  $c$  and  $d$  are neighbors  
 15 of  $a$  and  $b$ , there are two corresponding placement circles by Property 1. In fact, since any two edges of a Lombardi drawing of a 4-regular graph must enclose an angle of  $90^\circ$  and since  $a$  and  $b$  have “aligned tangents” due to being neighbors themselves, the two placement circles coincide and a situation as shown in Fig. 8 arises. In particular, this means that in any Lombardi drawing of  $G$  the four  
 20 vertices must be co-circular. It is easy to see that we cannot draw the missing circular arcs connecting  $c$  and  $d$ : any such arc must either lie completely inside or completely outside of the placement circle. Yet, the stubs for the two edges between  $c$  and  $d$  point inside at  $c$  and outside at  $d$ .  $\square$

The full proof for the following lemma is given in Appendix C.

25 **Lemma 4.** *Knots  $4_1$  and  $5_2$  do not have plane Lombardi drawings.*

*Sketch of Proof.* For knot  $4_1$ , the claim immediately follows from Lemma 3. For knot  $5_2$  (see Fig. 9) we can argue that all five vertices must be co-circular. Unlike knot  $4_1$  we can geometrically draw all edges of knot  $5_2$  as Lombardi arcs, see the non-plane drawing in Fig. 9b. However, by carefully considering the smooth  
 30 chain of arcs  $a - c - e - d - b$  and their radii, we can prove that this path must self-intersect in any Lombardi drawing, so the claim follows.  $\square$



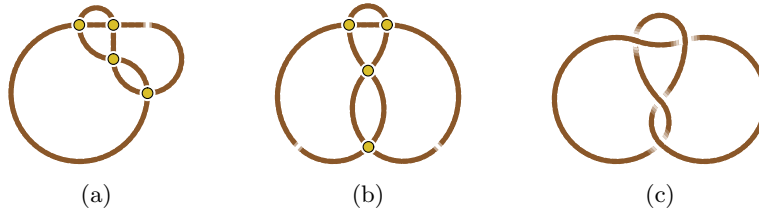


Fig. 10: Drawings of knot  $4_1$  which by Lemma 4 does not admit a plane Lombardi drawing. (a) A smooth orthogonal drawing of complexity 2, (b) a different plane 2-Lombardi drawing, and (c) a plane  $\varepsilon$ -angle Lombardi drawing.

As the above lemma shows, even very small knots may not have a plane Lombardi drawings. However, most knots with a small number of crossings are indeed plane Lombardi. In Fig. 17 in Appendix C, we provide plane Lombardi drawings of all knots with up to eight vertices except  $4_1$  and  $5_2$ . Most of these drawings can actually be obtained using the techniques from Sect. 2 and 3.

**Theorem 4.** *All prime knots with up to eight vertices other than  $4_1$  and  $5_2$  have plane Lombardi drawings.*

Note that Theorem 4 implies that each of these knots has a combinatorial embedding that supports a plane Lombardi drawing. It is not true, however, that any embedding admits a plane Lombardi drawing. In fact, the knot  $7_5$  has an embedding that cannot be drawn plane Lombardi; see details in Appendix C.

**Theorem 5.** *There exists an infinite family of prime knots and links that have embeddings that do not support plane Lombardi drawings.*

## 5 Plane 2-Lombardi Drawings of Knots and Links

Since not every knot admits a plane Lombardi drawing, we now consider plane 2-Lombardi drawings; see Fig. 10a for an example. Bekos et al [4] recently introduced *smooth orthogonal drawings of complexity  $k$* . These are drawings where every edge consists of a sequence of at most  $k$  circular arcs and axis-aligned segments that meet smoothly with horizontal or vertical tangents, and where at every vertex, each edge emanates either horizontally or vertically and no two edges emanate in the same direction. For the special case of 4-regular graphs, every smooth orthogonal drawing of complexity  $k$  is also a plane  $k$ -Lombardi drawing. Alam et al. [2] showed that every plane graph with maximum degree 4 can be redrawn as a plane smooth-orthogonal drawing of complexity 2. Their algorithm takes as input an orthogonal drawing produced by the algorithm of Liu et al. [12] and transforms it into a smooth orthogonal drawing of complexity 2. We show how to modify the algorithm by Liu et al., to compute an orthogonal drawing for a 4-regular plane multigraph and then use the algorithm by Alam et al. to transform it into a smooth orthogonal drawing of complexity 2. Details are given in Appendix D.

**Theorem 6.** *Every biconnected 4-regular plane multigraph  $G$  admits a plane 2-Lombardi drawing with the same embedding.*

## 6 Plane Near-Lombardi Drawings

Since not all knots admit a plane Lombardi drawing, in this section we relax  
 5 the perfect angular resolution constraint. We say that a knot (or a link) is *near-Lombardi* if it admits a drawing for every  $\varepsilon > 0$  such that

1. All edges are circular arcs,
2. Opposite edges at a vertex are tangent;
3. The angle between crossing pairs at each vertex is at least  $90^\circ - \varepsilon$ .

10 We call such a drawing a  $\varepsilon$ -*angle Lombardi drawing*. Note that a Lombardi drawing is essentially a 0-angle Lombardi drawing. For example, the knot  $4_1$  does not admit a plane Lombardi drawing, but it admits a plane  $\varepsilon$ -angle Lombardi drawing, as depicted in Fig. 10b.

Let  $\Gamma$  be an  $\varepsilon$ -angle Lombardi drawing of a 4-regular graph. If each angle described by the tangents of adjacent circular arcs at a vertex in  $\Gamma$  is exactly  $90^\circ + \varepsilon$   
 15 or  $90^\circ - \varepsilon$ , then we call  $\Gamma$  an  $\varepsilon$ -*regular Lombardi drawing*. Note that any Lombardi drawing is a 0-regular Lombardi drawing.

We first extend some of our results for plane Lombardi drawings to plane  
 20  $\varepsilon$ -angle Lombardi drawings. The following Lemma is a stronger version of Theorem 2. The full proof is given in Appendix E.

**Lemma 5.** *Let  $G = (V, E)$  be a biconnected 4-regular plane multigraph and let  $M$  and  $M'$  be the primal-dual multigraph pair for which  $G$  is the medial graph. If one of  $M$  and  $M'$  is simple, then  $G$  admits a plane  $\varepsilon$ -regular Lombardi drawing preserving its embedding for every  $0^\circ \leq \varepsilon < 90^\circ$ .*

25 *Sketch of Proof.* We first direct the edges such that every vertex has two incoming opposite edges and two outgoing opposite edges by We orient the edges around each face that belongs to  $M$  in counter-clockwise order. We use the same primal-dual circle packing approach as in Theorem 2 to obtain a drawing of  $G'$ ,  
 30 but instead of using the bisection of the lens region, we draw every edge with angles  $45^\circ + \varepsilon/2$  and  $45^\circ - \varepsilon/2$  around the source vertex in counter-clockwise order and around the target vertex in clockwise order. Whenever a vertex is removed, an incoming and an outgoing edge of it is substituted by a new edge between its neighbors, so the angles at the neighbors are compatible and the new edge can inherit the direction of the old edges.  $\square$

35 The following Lemmas is a stronger version of Lemma 1 and Theorem 1. Since the proofs do not rely on  $90^\circ$  angles, they can be immediately applied to the stronger version. A formal proof of Lemma 6 is given in Appendix E.

**Lemma 6.** *Let  $G = (V, E)$  be a 4-regular plane multigraph with a plane  $\varepsilon$ -angle Lombardi drawing  $\Gamma$ . Then, any lens multiplication  $G'$  of  $G$  also admits a plane  
 40  $\varepsilon$ -angle Lombardi drawing.*

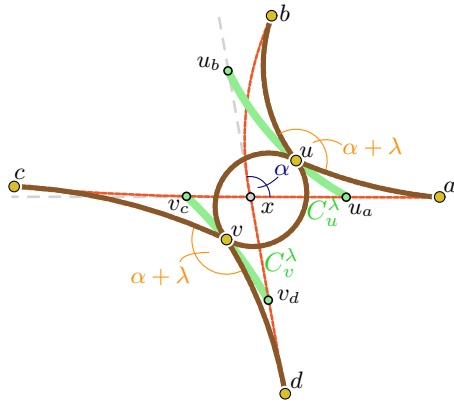


Fig. 11: The circular arc  $C_u^\lambda$  between  $u_a$  and  $u_b$  on the placement circles of  $u$  and the circular arc  $C_v^\lambda$  between  $v_c$  and  $v_d$  on the placement circles of  $v$ .

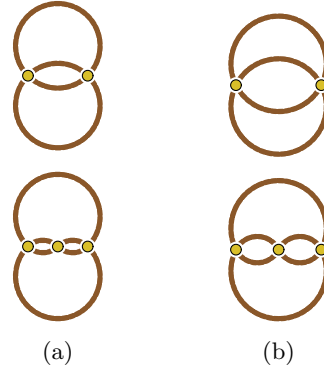


Fig. 12: The only biconnected 4-regular multigraphs with at most 3 vertices. (a) plane Lombardi and (b) plane  $\varepsilon$ -angle Lombardi drawings.

**Lemma 7.** *Let  $A$  and  $B$  be two 4-regular plane multigraphs with plane  $\varepsilon$ -angle Lombardi drawings. Let  $a$  be an edge of  $A$  and  $b$  an edge of  $B$ . Then the composition  $A + B$  obtained by connecting  $A$  and  $B$  along edges  $a$  and  $b$  admits a plane  $\varepsilon$ -angle Lombardi drawing.*

5 Let  $G = (V, E)$  be a 4-regular plane multigraph and let  $x \in V$  with edges  $(x, a)$ ,  $(x, b)$ ,  $(x, c)$ , and  $(x, d)$  in counter-clockwise order. A *lens extension* of  $G$  is a 4-regular plane multigraph that is obtained by removing  $x$  and its incident edges from  $G$ , and adding two vertices  $u$  and  $v$  to  $G$  with two edges between  $u$  and  $v$  and the edges  $(u, a)$ ,  $(u, b)$ ,  $(v, c)$ ,  $(v, d)$ . Informally, that means  
10 that a vertex is substituted by a lens.

**Lemma 8.** *Let  $G = (V, E)$  be a 4-regular plane multigraph with a plane  $\varepsilon$ -angle Lombardi drawing  $\Gamma$ . Then, any lens extension of  $G$  admits a plane  $(\varepsilon + \varepsilon')$ -angle Lombardi drawing for every  $\varepsilon' > 0$ .*

*Sketch of Proof.* Let  $x \in V$  be the vertex that we want to perform the lens  
15 extension on, such that we get the edges  $(u, a)$ ,  $(u, b)$ ,  $(v, c)$ ,  $(v, d)$  in the obtained graph  $G'$ . Let  $\alpha$  be the angle between the tangents of  $(x, a)$  and  $(x, b)$  at  $x$  in  $\Gamma$ . Since  $\Gamma$  is a plane  $\varepsilon$ -angle Lombardi drawing, we have that  $\alpha \leq 90^\circ + \varepsilon$ . Further, the angle between the tangents of  $(x, c)$  and  $(x, d)$  at  $x$  in  $\Gamma$  is also  $\alpha$ , while the angles between the tangents of  $(x, b)$  and  $(x, c)$  at  $x$  and between the tangents  
20 of  $(x, d)$  and  $(x, a)$  at  $x$  are both  $180^\circ - \alpha$ . We apply the Möbius-transformation on  $\Gamma$  that maps the edges  $(x, a)$  and  $(x, d)$  to straight-line segments and  $a$  lies on the same  $y$ -coordinate and to the right of  $x$ ; hence,  $d$  lies strictly below  $x$ .

We aim to place  $v$  such that the angle between the arcs  $(v, c)$  and  $(v, d)$  is  $\alpha + \lambda$  for some  $0 < \lambda \leq \varepsilon'$ , which we will show how to choose later. We have fixed

ports at  $c$  and  $d$  and a fixed angle  $\alpha + \lambda$  at  $v$ . According to Property 1, all possible positions of  $v$  lie on a circle through  $c$  and  $d$ . Note that the circle through  $c$ ,  $d$ , and  $x$  describes all possible positions of neighbors of  $c$  and  $d$  with angle  $\alpha$ . Since the desired angle gets larger, the position circle for  $v$  contains a point  $v_d$  on the straight-line edge  $(x, d)$  and a point  $v_c$  on the half-line starting from  $x$  with the angle of the port used by the arc  $(x, c)$ ; see Fig. 11. We denote by  $C_v^\lambda$  the circular arc between  $v_c$  and  $v_d$  on the placement circle of  $v$  that gives the angle  $\alpha + \lambda$  at  $v$ . We use the same construction for  $u$  to obtain the circular arc  $C_u^\lambda$  between  $u_a$  and  $u_b$ . Since the drawing of  $G$  is plane, there exists some non-empty region in which we can move  $x$ , such that the arcs  $(x, a)$ ,  $(x, b)$ ,  $(x, c)$ ,  $(x, d)$  are drawn with the same ports at  $a, b, c, d$  and do not cross any other edge of the drawing. We choose  $\lambda$  as the largest value with  $0 < \lambda \leq \varepsilon'$  such that the two circular arcs  $C_u$  and  $C_v$  lie completely inside this region.

We show how to find a pair of points on  $C_v^\lambda$  and  $C_u^\lambda$  such that we can connect them via a lens in Appendix E □

**Lemma 9.** *Every 4-regular plane multigraph with at most 3 vertices admits a plane  $\varepsilon$ -regular Lombardi drawing for every  $0 \leq \varepsilon < 90^\circ$ .*

*Proof.* There are only two 4-regular multigraphs with at most 3 vertices and each of them has a plane Lombardi drawing as depicted in Fig. 12a. For some  $0^\circ < \varepsilon < 90^\circ$ , we can obtain a plane  $\varepsilon$ -regular Lombardi drawing by simply making the circular arcs larger or smaller, as depicted in Fig. 12b. □

We are now ready to present the main result of this section. The proof boils down to a large case distinction using the tools developed in the previous discussion. We split the original graph into biconnected components and then use Lemma 9 and 5 as base cases. With the help of lens extensions, lens multiplications, and knot sums we can combine the “near-Lombardi” drawings of the biconnected graphs to generate an “near-Lombardi” drawing of the original graph. As a consequence, every knot is near-Lombardi. The full proof is given in Appendix E.

**Theorem 7.** *Let  $G = (V, E)$  be a biconnected 4-regular plane multigraph and let  $\varepsilon > 0$ . Then  $G$  admits a plane  $\varepsilon$ -angle Lombardi drawing.*

*Acknowledgements.* Research for this work was initiated at Dagstuhl Seminar 17072 *Applications of Topology to the Analysis of 1-Dimensional Objects* which took place in February 2017. We thank Benjamin Burton for bringing the problem to our attention and Dylan Thurston for helpful discussion.

## References

1. Knot drawing in Knot Atlas. [http://katlas.org/wiki/Printable\\_Manual#Drawing\\_Planar\\_Diagrams](http://katlas.org/wiki/Printable_Manual#Drawing_Planar_Diagrams). Accessed: 2017-06-08.
2. M. J. Alam, M. A. Bekos, M. Kaufmann, P. Kindermann, S. G. Kobourov, and A. Wolff. Smooth orthogonal drawings of planar graphs. In P. A. and V. A., editors, *Proc. 13th Lat. Am. Symp. Theoret. Inform. (LATIN'14)*, number 8392 in LNCS, pages 144–155. Springer-Verlag Berlin Heidelberg, 2014.
3. J. W. Alexander and G. B. Briggs. On types of knotted curves. *Ann. Math.*, 28:562–586, 1927.
4. M. A. Bekos, M. Kaufmann, S. G. Kobourov, and A. Symvonis. Smooth orthogonal layouts. In W. Didimo and M. Patrignani, editors, *Proc. 20th Int. Symp. Graph Drawing (GD'12)*, volume 7704 of *Lecture Notes Comput. Sci.*, pages 150–161. Springer, 2013.
5. G. R. Brightwell and E. R. Scheinerman. Representations of planar graphs. *SIAM J. Discrete Math.*, 6(2):214–229, 1993.
6. P. R. Cromwell. *Knots and links*. Cambridge University Press, 2004.
7. C. A. Duncan, D. Eppstein, M. T. Goodrich, S. G. Kobourov, and M. Löffler. Planar and poly-arc Lombardi drawings. In M. van Kreveld and B. Speckmann, editors, *Proc. 19th Int. Symp. Graph Drawing (GD'11)*, volume 7034 of *Lecture Notes Comput. Sci.*, pages 308–319. Springer, 2012.
8. C. A. Duncan, D. Eppstein, M. T. Goodrich, S. G. Kobourov, and M. Nöllenburg. Lombardi drawings of graphs. *J. Graph Algorithms Appl.*, 16(1):37–83, 2012.
9. D. Eppstein. Planar Lombardi drawings for subcubic graphs. In W. Didimo and M. Patrignani, editors, *Proc. 20th Int. Symp. Graph Drawing (GD'12)*, volume 7704 of *Lecture Notes Comput. Sci.*, pages 126–137. Springer, 2013.
10. D. Eppstein. A Möbius-invariant power diagram and its applications to soap bubbles and planar Lombardi drawing. *Discrete Comput. Geom.*, 52:515–550, 2014.
11. L. H. Kauffman. *On Knots*, volume 115 of *Annals of Mathematical Studies*. Princeton University Press, 1987.
12. Y. Liu, A. Morgana, and B. Simeone. A linear algorithm for 2-bend embeddings of planar graphs in the two-dimensional grid. *Discrete Appl. Math.*, 81(1–3):69–91, 1998.
13. C. Livingston. *Knot Theory*, volume 24 of *The Carus Mathematical Monographs*. Mathematical Association of America, 1993.
14. D. Rolfsen. *Knots and Links*. American Mathematical Soc., 1976.
15. R. G. Scharein. *Interactive Topological Drawing*. PhD thesis, Department of Computer Science, The University of British Columbia, 1998.
16. H. Schubert. Sitzungsbericht. *Heidelberger Akad. Wiss., Math.-Naturwiss. Klasse, 3. Abhandlung*, 1949.
17. W. T. Tutte. How to draw a graph. *Proc. London Math. Soc.*, 13(3):743–768, 1963.

## A Additional Material for Section 2

**Theorem 1.** *Let  $A$  and  $B$  be two 4-regular multigraphs with plane Lombardi drawings. Let  $a$  be an edge of  $A$  and  $b$  an edge of  $B$ . Then the knot sum  $A + B$ , obtained by connecting  $A$  and  $B$  along edges  $a$  and  $b$ , admits a plane Lombardi drawing.*

*Proof.* We first apply a Möbius transformation to the plane Lombardi drawings of  $A$  and  $B$  so that in the resulting drawings the given edges  $a$  and  $b$  are drawn as straight edges passing through the point at infinity, i.e., they are complements of line segments on an infinite-radius circle; see Fig. 3. Next, we rotate and align both of these drawings so that edges  $a$  and  $b$  are collinear and the subdrawings obtained by removing edges  $a$  and  $b$  do not intersect. In the final step, we remove both  $a$  and  $b$  and reconnect their vertices by two new edges  $c$  and  $d$  connecting the two drawings, one being a line segment and the other passing through infinity. Since Möbius transformations preserve planarity and Lombardiness and our construction does not introduce any edge crossings, the resulting drawing is a plane Lombardi drawing. Another Möbius transformation may be applied to remove the edge through infinity.  $\square$

**Lemma 1.** *Let  $G = (V, E)$  be a 4-regular plane multigraph with a plane Lombardi drawing  $\Gamma$ . Then, any lens multiplication  $G'$  of  $G$  also admits a plane Lombardi drawing.*

*Proof.* Let  $f$  be a lens in  $\Gamma$  spanned by two vertices  $u$  and  $v$ . We denote the two edges bounding the lens as  $e_1$  and  $e_2$ . The angle between  $e_1$  and  $e_2$  in both end-vertices is  $90^\circ$ . We define the bisecting circular arc  $b$  of  $f$  as the unique circular arc connecting  $u$  and  $v$  with an angle of  $45^\circ$  to both  $e_1$  and  $e_2$ ; see Fig. 4.

Let  $p$  be the midpoint of  $b$ . If we draw circular arcs from both  $u$  and  $v$  to  $p$  that have the same tangents as  $e_1$  and  $e_2$  in  $u$  and  $v$ , then these four arcs meet at  $p$  forming angles of  $90^\circ$ . Furthermore, each such arc lies inside lens  $f$  and hence does not cross any other arc of  $\Gamma$ . The resulting drawing is thus a plane Lombardi drawing of a 4-regular multigraph that is derived from  $G$  by subdividing the lens  $f$  with a new degree-4 vertex.

By repeating this construction inside the new lenses, we can create plane Lombardi drawings that replace lenses by chains of smaller lenses.  $\square$

## B Additional Material for Section 3

### B.1 Proof of Theorem 2

**Theorem 2.** *Let  $G = (V, E)$  be a biconnected 4-regular plane multigraph and let  $M$  and  $M'$  be the primal-dual multigraph pair for which  $G$  is the medial graph. If one of  $M$  and  $M'$  is simple, then  $G$  admits a plane Lombardi drawing preserving its embedding.*

*Proof.* Assume w.l.o.g. that  $M$  is simple. If  $M$  (and hence also  $M'$ ) is polyhedral, then  $G$  admits a plane Lombardi drawing  $\Gamma$  by Eppstein [9].

It remains to show that  $\Gamma$  preserves the embedding of  $G$ . The drawing  $\Gamma$  is constructed in the following way: Consider a primal-dual circle packing  $C(M, M')$  of  $(M, M')$  which exists due to Brightwell and Schreinerman [5]. The plane Lombardi drawing  $\Gamma$  of  $G$  then is essentially the Voronoi diagram of  $C(M, M')$ . As the combinatorial embedding of  $M$  and  $M'$  is unique up to homeomorphism on the sphere, there exists a Möbius transformation  $\tau$  such that the circle packing  $\tau(C(M, M'))$  has the same unbounded face as  $D(M, M')$ . Hence,  $\Gamma$  is a plane Lombardi drawing of  $G$  that preserves its combinatorial embedding.

Now assume that  $M$  is not 3-connected. As a first step, we iteratively extend  $M = M_0$  by adding  $p$  edges until we obtain a polyhedral graph  $M_p$ . During this process, we also iteratively adapt the dual graph and the medial graph; see Fig. 13 for an illustration. Let  $M_{i+1}$  be the graph obtained from  $M_i$  by adding edge  $e$  to  $M_i$ . The edge  $e$  splits a face  $f$  of  $M_i$  with at least four incident vertices into two faces  $f_1$  and  $f_2$  with at least three incident vertices each. In  $M'_i$ , the according vertex  $f'$  is split into two vertices  $f'_1$  and  $f'_2$ . The edges incident to  $f'$  are partitioned into edges incident to  $f'_1$  and  $f'_2$  and an additional edge between  $f'_1$  and  $f'_2$  is added. In  $G_i$ , the edges inside the face  $f$  of  $M_i$  form a cycle that connects every pair of edges in  $M_i$  that is incident along the boundary of  $f$ . When  $e$  is added, exactly two edges  $g_1, g_2$  of  $G_i$  are intersected by  $e$ . To obtain  $G_{i+1}$ , the edges  $g_1$  and  $g_2$  are replaced by four new edges, where each new edge has the new crossing between  $e$  and  $(f'_1, f'_2)$  as one endpoint and one of the four endpoints of  $g_1$  and  $g_2$ , respectively, as the other endpoint.

In the second step, we apply the result of Eppstein [9] to obtain a plane Lombardi drawing  $\Gamma_p$  of  $G_p$  together with a primal-dual circle packing  $C(M_p, M'_p)$ . Before going into the third step, the iterative removal of the edges that were added in the first step, let us consider the structure obtained from the second step in more detail; see Fig. 13 (bottom right) and Fig. 5c. For an edge  $g$  of  $G_p$ , consider the unique vertex  $m(g) \in M_p$  that lies in a cell of  $G_p$  incident to  $g$ . Note that  $g$  has its endpoints on two edges incident to  $m(g)$  and adjacent in their order around  $m(g)$ . Let these edges be  $(m(g), m_1(g))$  and  $(m(g), m_2(g))$ , respectively. Let  $d(g), d_1(g),$  and  $d_2(g)$  be the disks in  $C(M_p)$  corresponding to  $m(g), m_1(g),$  and  $m_2(g)$ , respectively. Then in  $\Gamma_p$ , the circular arc  $c(g)$  corresponding to  $g$  lies in the interior<sup>2</sup> of the disk  $d(g)$  and has its endpoints on the touching points of  $d(g)$  with  $d_1(g)$  and  $d_2(g)$ , respectively. These touching points are consecutive along the boundary of  $d(g)$ . Further, there is a disk  $d'(g)$  in  $C(M'_p)$  whose boundary intersects the boundary of  $d(g)$  exactly in the endpoints of  $c(g)$ . The intersection of  $d(g)$  and  $d'(g)$  contains  $c(g)$  in its interior. The circles  $\partial d(g)$  and  $\partial d'(g)$  intersect with right angles and  $c(g)$  bisects the angles at both intersections. We call  $d(g) \cap d'(g)$  the *lens region*  $\ell(g)$  of  $g$ . For any two edges  $g_1$  and  $g_2$  of  $\Gamma_p$ , the according lens regions  $\ell(g_1)$  and  $\ell(g_2)$  are interior-disjoint. The lens regions of the edges incident to the face in  $\Gamma_p$  corresponding

<sup>2</sup> Here, *interior* is meant w.r.t. the circle packing. Note that a circle could also be inverted, that is, contain the unbounded face.

to  $m(g)$  cover the whole boundary of  $d(g)$  and the endpoints of those regions appear in the same cyclic order as the according edges in  $M_p$ .

In the third step, we iteratively remove the edges that were added in the first step, by this constructing a sequence of plane Lombardi drawings  $\Gamma_i$  for  $G_i$ , for  $i = p - 1, \dots, 0$ ; see Fig. 14 for an example. For any edge  $g$  of  $G_i$ , consider the unique vertex  $m(g) \in M_i$  that lies in a cell of  $\Gamma_i$  incident to  $g$ , with endpoints on edges  $(m(g), m_1(g))$  and  $(m(g), m_2(g))$  of  $M_i$ , respectively. Let  $d(g)$ ,  $d_1(g)$ , and  $d_2(g)$  be the disks in  $C(M_p)$  corresponding to  $m(g)$ ,  $m_1(g)$ , and  $m_2(g)$ , respectively, and let  $c(g)$  be the circular arc in  $\Gamma_i$  corresponding to  $g$ . We keep the following invariants for all edges  $g$  of the drawing  $\Gamma_i$ : (i)  $c(g)$  lies in the disk  $d(g)$  and has its endpoints on the touching points of  $d(g)$  with  $d_1(g)$  and  $d_2(g)$ , respectively. (ii) There is a disk  $d'(g)$  whose boundary intersects the boundary of  $d(g)$  exactly in  $d(g) \cap d_1(g)$  and  $d(g) \cap d_2(g)$ , such that  $c(g)$  bisects one of the two regions  $d(g) \cap d'(g)$  and  $d(g) \cap \mathbb{R}^2 \setminus d'(g)$ , which we call its lens region  $\ell(g)$ . (iii) For any two edges  $g_1$  and  $g_2$  of  $G_i$ , the lens regions  $\ell(g_1)$  and  $\ell(g_2)$  are interior-disjoint. (iv) The lens regions of the edges incident to the face in  $D(G_i)$  corresponding to  $m(g)$  cover the whole boundary of  $d(g)$  and the endpoints of those regions appear in the same cyclic order as the according edges in  $D(M_i)$ .

Obviously, those invariants are fulfilled by  $\Gamma_p$ . Hence, assume that they are also fulfilled for  $\Gamma_{i+1}$ , and consider the removal of the edge  $e = (v_1, v_2)$  from  $M_{i+1}$  to obtain  $M_i$ . In the medial graph  $G_{i+1}$ , the edge  $e$  corresponds to four edges sharing the vertex corresponding to  $e$ , and there are two unique faces corresponding to  $v_1$  and  $v_2$ , respectively. Each of those has two of the edges of  $G_{i+1}$  corresponding to  $e$  as consecutive edges along the face. Let  $g_1$  and  $g_2$  be those consecutive incident edges on the face of  $G_{i+1}$  corresponding to  $v_1$ . Note that their non-shared endpoints lie on the edges  $(v_1, v_3)$  and  $(v_1, v_4)$ , respectively, where  $v_3$  and  $v_4$  are consecutive in the cyclic order around  $v_1$  in  $M_i$ . Further, note that, when removing  $e$  from  $M_{i+1}$ , we have to replace  $g_1$  and  $g_2$  by an edge  $g$  connecting their non-shared endpoints. For every  $j \in \{1, 2, 3, 4\}$ , let  $d(v_j)$  be the disk of  $C(M_p)$  that corresponds to the vertex  $v_j$  of  $M_i \subset M_p$  (note that with the notation from the invariants,  $d(v_1) = d(g_1) = d(g_2)$ ). Next, consider  $c(g_1)$  and  $c(g_2)$  in the drawing  $\Gamma_{i+1}$ . By our invariants,  $c(g_1)$  and  $c(g_2)$  lie in their lens regions  $\ell(g_1)$  and  $\ell(g_2)$ , which are consecutive along the boundary of  $d(v_1)$ . The only common point of  $\ell(g_1)$  and  $\ell(g_2)$  is the touching point of  $d(v_1)$  and  $d(v_2)$ . The other endpoints of  $c(g_1)$  and  $c(g_2)$  are the touching points  $d(v_1) \cap d(v_3)$  and  $d(v_1) \cap d(v_4)$ , respectively. Further, the boundary of  $d(v_1)$  is completely covered by lens regions which are all pairwise non-intersecting and bounded by circles intersecting  $\partial d(v_1)$  in right angles. We replace  $c(g_1)$  and  $c(g_2)$  by the circular arc  $c(g)$  that has as its endpoints at the touching points  $d(v_1) \cap d(v_3)$  and  $d(v_1) \cap d(v_4)$  and is tangent to  $c(g_1)$  and  $c(g_2)$ , respectively, in its endpoints. We define the lens region  $\ell(g)$  as the unique region that contains  $\ell(g_1)$  and  $\ell(g_2)$  and is the intersection of  $d(v_1)$  with the (according side of the) unique disk  $d'(g)$  for which  $\partial d'(g)$  intersects  $\partial d(v_1)$  at a right angle in the endpoints of  $c(g)$ ; see Fig. 6.

Note that  $\ell(g)$  does not intersect the interior of any other lens region: for the lens regions outside  $d(v_1)$ , this is trivial. For the ones inside  $d(v_1)$ , it follows



from continuous transformation of the bounding circle  $\partial d'(g)$  to the bounding circle of the other lens. Hence, after repeating the analogous construction for the two other edges in  $G_{i+1}$  needed to be replaced when removing  $e$  from  $M_{i+1}$ , namely the ones that are incident to the face corresponding to  $v_2$  in  $D(G_{i+1})$ , we obtain a plane Lombardi drawing  $\Gamma_i$  that again fulfills our four invariants, which completes the proof.  $\square$

**B.2 Drawing Knots  $5_1$ ,  $6_2$ ,  $7_7$ , and  $8_{18}$  via Circle Packing**

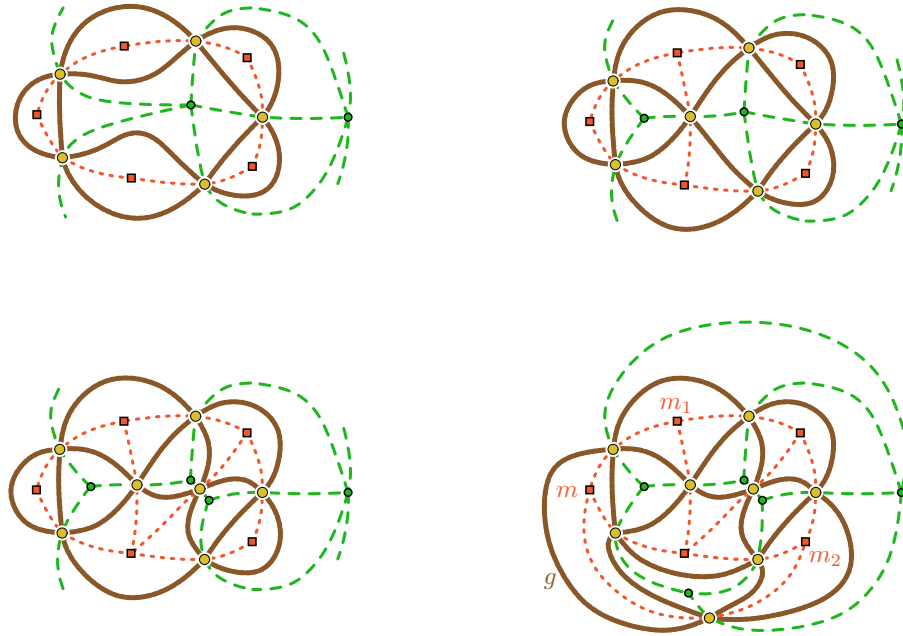


Fig. 13: Extension of the primal graph (dotted) of knot  $5_1$  to the square pyramid and its dual (dashed). The medial graph in the top right is the knot  $6_2$ , the medial graph in the bottom left is the knot  $7_7$ , and the medial graph in the bottom right is the knot  $8_{18}$ .

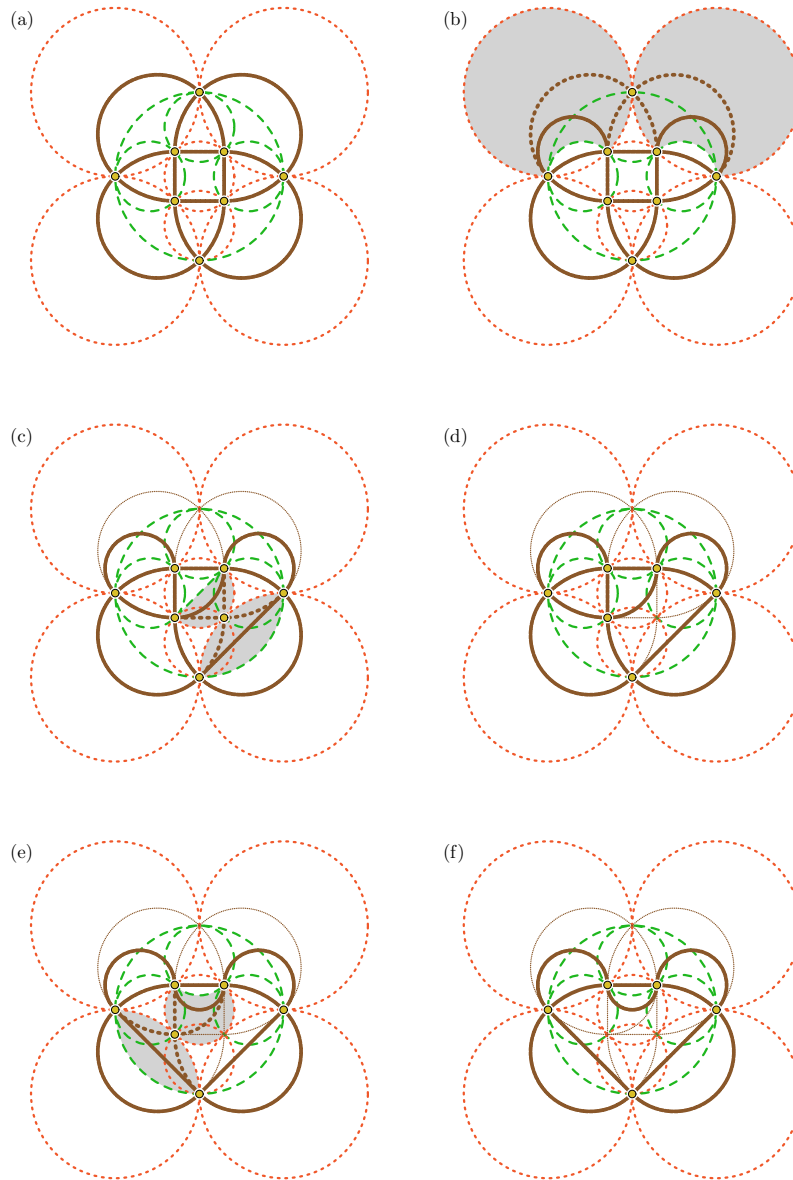


Fig. 14: (a) A circle packing for the square pyramid (dotted) and its dual (dashed), and a plane Lombardi drawing for the medial graph  $8_{18}$  (solid); (b) eliminating an edge of the primal and the plane Lombardi drawing of  $7_7$ ; (c) eliminating an edge of the primal; (d) the plane Lombardi drawing of  $6_2$ ; (e) eliminating an edge of the primal; (f) the plane Lombardi drawing of  $5_1$ .

### C Additional Material for Section 4

**Lemma 4.** *Knots  $4_1$  and  $5_2$  do not have plane Lombardi drawings.*

*Proof.* For knot  $4_1$ , the claim immediately follows from Lemma 3.

Knot  $5_2$  again has the property that all five vertices must be co-circular in any Lombardi drawing. To see this, we first consider the four vertices  $a, b, c, d$  in Fig. 9. Regardless of the placement of  $a$  and  $b$ , we observe that  $c$  and  $d$  are both adjacent to  $a$  and  $b$  and need to enclose an angle of  $90^\circ$  in the triangular face with  $a$  and  $b$ . This situation was already discussed in Lemma 3 and yields a circle  $C$  containing  $a, b, c, d$ ; see Fig. 8. The final vertex,  $e$ , is adjacent to  $c$  and  $d$  so that we can determine the placement circle for  $e$  with respect to  $c$  and  $d$ . As we know from Lemma 3, the two arc stubs of  $d$  to be connected with  $e$  form angles of  $45^\circ$  with  $C$  and point outwards. Conversely, the two arc stubs of  $c$  form angles of  $45^\circ$  with  $C$  and point inwards. If we take any point  $p$  on  $C$  and draw circular arcs from the stubs of  $c$  and  $d$  to  $p$ , the four arcs meet at  $90^\circ$  angles in  $p$ . These are precisely the angles required at vertex  $e$  and hence  $C$  is in fact the unique placement circle for  $e$  by Property 1. This implies that actually all five vertices of  $5_2$  must be co-circular in any Lombardi drawing.

Unlike knot  $4_1$ , it is geometrically possible to draw all edges as Lombardi arcs; see Fig. 9b. However, as we will show, no plane Lombardi drawing of knot  $5_2$  exists. By an appropriate Möbius transformation, we may assume that all five vertices are collinear on a circle of infinite radius. Moreover, to avoid crossings, the order along the line is either  $a, b, c, e, d$  or  $a, b, d, e, c$  (modulo cyclic shifts and reversals). Since both cases are symmetric, we restrict the discussion to the first one. As a further simplification, we initially assume that  $a$  and  $b$  are placed on the same position such that the lens between  $a$  and  $b$  collapses; see Fig. 15.

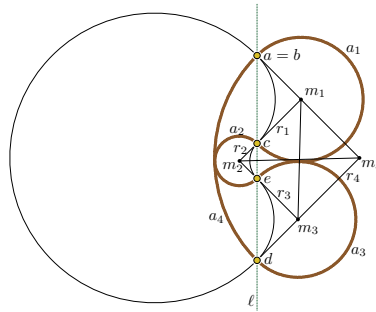


Fig. 15: Knot  $5_2$  has no plane Lombardi drawing.

This drawing consists of two intertwined 4-cycles, which intersect the line  $\ell$  at angles of  $45^\circ$ . We argue that the 4-cycle depicted in Fig. 15 cannot be drawn as a simple cycle without self intersections. We consider the four centers  $m_1, m_2, m_3, m_4$  of the circular arcs  $a_1, a_2, a_3, a_4$  and their radii  $r_1, r_2, r_3, r_4$ .

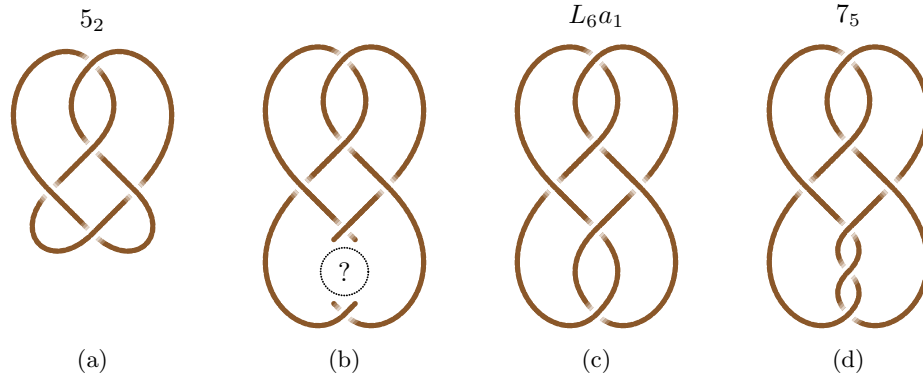


Fig. 16: A family of non-Lombardi knots and links.

Due to the fact that adjacent arcs meet on  $\ell$  at an angle of  $45^\circ$  and have the same tangent, the four centers form the corners of a rectangle  $R$  with side lengths  $r_1 + r_2$  and  $r_3 + r_2$ . We can further derive that  $r_4 - r_3 = r_1 + r_2$ . Let  $\delta$  be the length of a diagonal of  $R$ . For the arcs  $a_1$  and  $a_3$  to be disjoint, we require  $\delta > r_1 + r_3$ . For  $a_2$  and  $a_4$  to be disjoint, we require  $\delta < r_4 - r_2$ . But since  $r_4 - r_2 = r_1 + r_3$ , this is impossible and the 4-cycle must self-intersect.

Finally, if we move  $b$  by some  $\varepsilon > 0$  away from  $a$  and towards  $c$ , this will only decrease the radius  $r_4$  and thus introduce proper intersections in the drawing. Thus, knot  $5_2$  has no plane Lombardi drawing.  $\square$

**Theorem 5.** *There exists an infinite family of prime knots and links that have embeddings that do not support plane Lombardi drawings.*

*Proof.* Consider again the knot  $5_2$  (Fig. 16a). By Lemma 4, it has no Lombardi drawing. We claim that if we duplicate the bottom vertex and detach the two copies completely, the resulting graph (using four stubs to ensure the correct angular resolution) still has no plane Lombardi drawing (Fig. 16b). As a result, we can construct an infinite family of forms of knots and links without plane Lombardi drawings. The first two smallest members of this family are the link  $L_6 a_1$ , consisting of two interlinked figure-8's (Fig. 16c), and the knot  $7_5$  (Fig. 16d). Note, however, that  $7_5$  has a different embedding that does have a plane Lombardi drawing; see Fig. 17.  $\square$

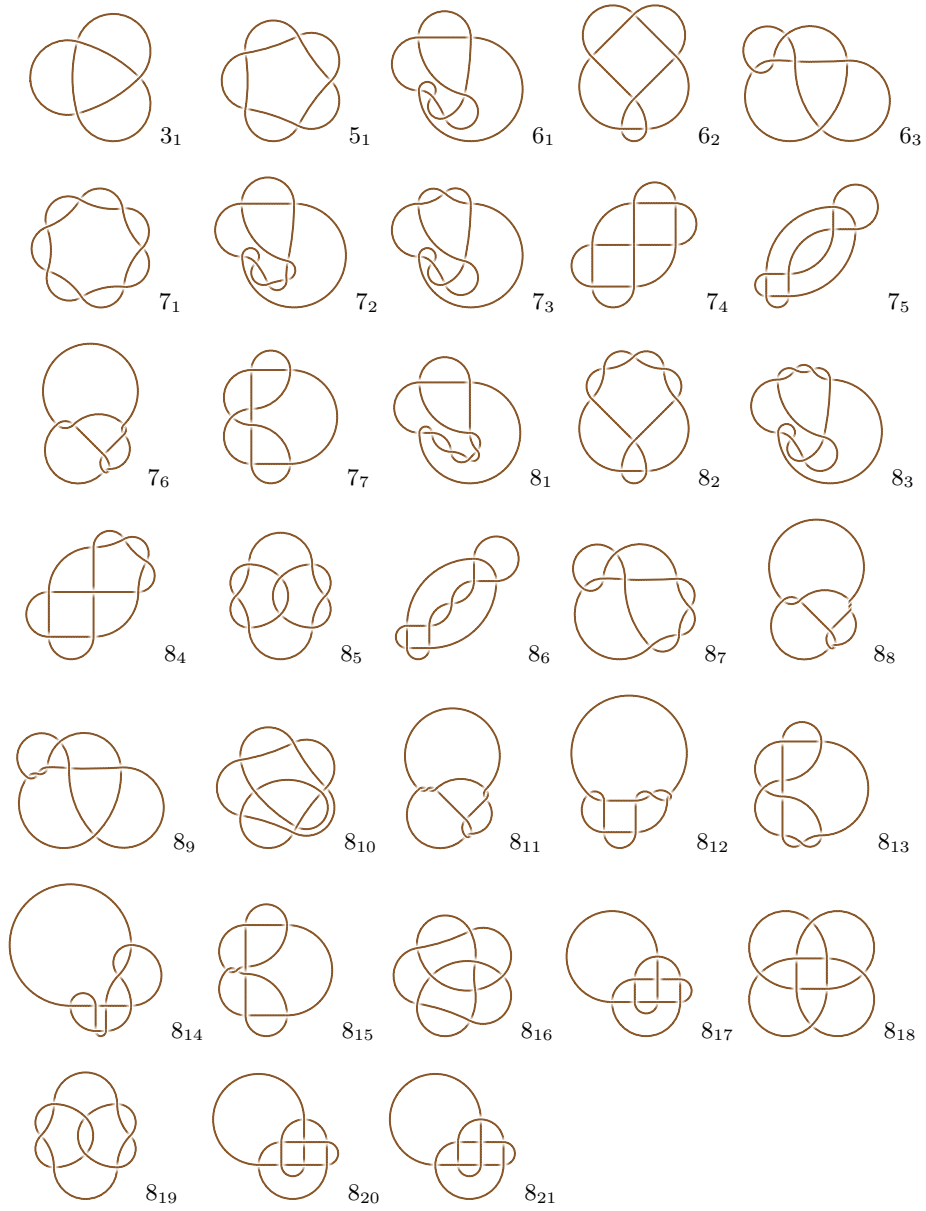


Fig. 17: Plane Lombardi drawings of all prime Lombardi knots up to 8 vertices.

## D Omitted Proofs from Section 5

**Theorem 6.** *Every biconnected 4-regular plane multigraph  $G$  admits a plane 2-Lombardi drawing with the same embedding.*

*Proof.* The algorithm of Alam et al. [2] takes as input an orthogonal drawing produced by the algorithm of Liu et al. [12] and transforms it into a smooth orthogonal drawing of complexity 2. The drawings by Liu et al. have the property that every edge consists of at most 3 segments (except at most one edge that has 4 segments), and it contains no *S-shapes*, that is, it contains no edge that consists of 3 segments where the bends are in opposite direction. To show this theorem, we only have to show that we can apply the algorithm of Liu et al. to 4-regular plane multigraphs to produce a drawing with the same property.

Liu et al. first choose two vertices  $s$  and  $t$  and compute an *st-order* of the input graph. An *st-order* is an ordering ( $s = 1, 2, \dots, n = t$ ) of the vertices such that every  $j$  ( $2 < j < n - 1$ ) has neighbors  $i$  and  $k$  with  $i < j < k$ . We can obtain an *st-order* for a multigraph by removing any duplicate edges. Liu et al. then direct all edges according to the *st-order* from a vertex with lower *st-number* to a vertex with higher *st-number*.

According to the rotation system implied by the embedding of the input graph, Liu et al. then assign a port to every edge around a vertex such that every vertex (except  $t$ ) has an outgoing edge at the top port, every vertex (except  $s$ ) has an incoming edge at the top port, every vertex has an outgoing edge at the right port if and only if it has at least 2 outgoing edges, and every vertex has an incoming edge at the left port if and only if it has at least 2 incoming edges. They further make sure the edge that uses the bottom port at  $s$  is incident to the vertex  $r$  with *st-number* 2, and that the edge  $(s, t)$ , if it exists, uses the left port at  $s$  and the top port at  $t$ ; this edge is the only one drawn with 4 segments, but can still be transformed into a smooth orthogonal edge of complexity 2 by Alam et al. . They place the vertices  $s$  and  $r$  on the  $y$ -coordinate 2 and every other vertex on the  $y$ -coordinates equal to their *st-number*. The shape of the edges is then implied by the assigned ports at their incident vertices. By placing vertices that share an edge with a bottom port and a top port above each other, there can be no S-shapes with two vertical segments, but there can still be S-shapes with two horizontal segments if an edge uses a left port and a right port. To eliminate these S-shapes, they consider sequences of S-shapes, that is, paths in the graphs that are drawn only with S-shapes, and move the vertices vertically such that they all lie on the same  $y$ -coordinate. Up to the elimination of S-shapes, every step of the algorithm can immediately be applied to multigraphs. We choose  $s$  and  $t$  as vertices on the outer face of the given embedding such that the edge  $(s, t)$  exists. We claim that then no multi-edge can be drawn as an S-shape.

Let  $u$  and  $v$  be two vertices in  $G$  with at least two edges  $e_1$  and  $e_2$  between them. W.l.o.g., let  $u$  have a lower *st-number* than  $v$ . Then both  $e_1$  and  $e_2$  are directed from  $u$  to  $v$ . If  $u = s$  and  $v = r$ , then both vertices are placed on the same  $y$ -coordinate, so there can be no S-shape between them. If  $u = s$  and  $v = t$ , then there is an edge that uses the left port at  $u$  and the top port at  $v$ ; since all

multi-edges have to be consecutive around  $u$  and  $v$ , there can be no edge between them that uses a left port and a right port. Otherwise, assume that  $e_2$  is the successor of  $e_1$  in counter-clockwise order around  $u$  (and hence the predecessor of  $e_1$  in counter-clockwise order around  $v$ ). If  $e_1$  uses the right port at  $u$  and the left port at  $v$ , then  $e_2$  has to use the top port at  $v$ , which cannot occur by the port assignment. If  $e_1$  uses the left port at  $u$  and the right port at  $v$ , then  $e_2$  has to use the bottom port at  $u$ , which also cannot occur by the port assignment. Thus, neither  $e_1$  nor  $e_2$  is drawn as an S-shape and every sequence of S-shapes consists only of simple edges. Hence, we can use the algorithm of Liu et al. to produce an orthogonal drawing with the desired property for every 4-regular plane multigraph and then use the algorithm of Alam et al. to transform it into a smooth complexity drawing of complexity 2 which is also a plane 2-Lombardi drawing.  $\square$

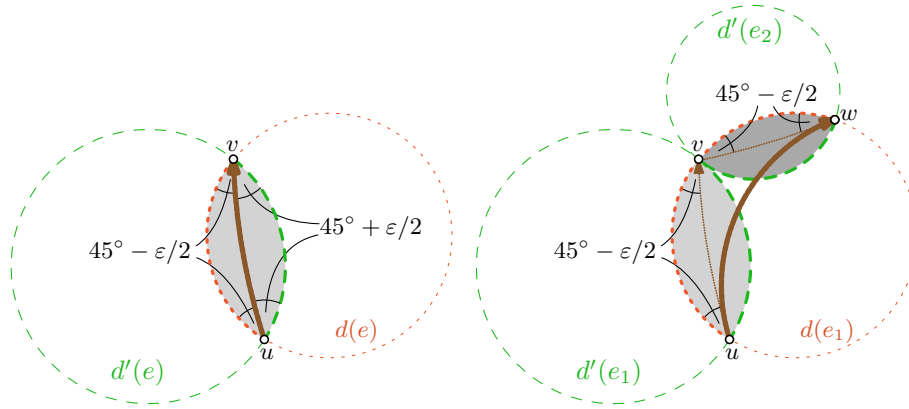
## E Omitted Proofs from Section 6.

**Lemma 5.** *Let  $G = (V, E)$  be a biconnected 4-regular plane multigraph and let  $M$  and  $M'$  be the primal-dual multigraph pair for which  $G$  is the medial graph. If one of  $M$  and  $M'$  is simple, then  $G$  admits a plane  $\varepsilon$ -regular Lombardi drawing preserving its embedding for every  $0^\circ \leq \varepsilon < 90^\circ$ .*

*Proof.* We use the same algorithm as for the proof of Theorem 2 with a slight modification. We first seek to direct the edges such that every vertex has two incoming opposite edges and two outgoing opposite edges. Let  $M$  and  $M'$  be the primal-dual pair corresponding to the medial graph  $G$ . Every face in  $G$  corresponds to a vertex either in  $M$  or in  $M'$ ; we say that the face *belongs to*  $M$  or  $M'$ . We orient the edges around each face that belongs to  $M$  in counter-clockwise order. Every edge in  $G$  lies between a face that belongs to  $M$  and a face that belongs to  $M'$ , so this gives a unique orientation for every edge. Further, the faces around any vertex belong to  $M$ , to  $M'$ , to  $M$ , and to  $M'$  in counter-clockwise order. Hence, the edges around any vertex are outgoing, incoming, outgoing, and incoming in counter-clockwise order, which gives us the wanted edge orientation.

We use the same primal-dual circle packing approach to obtain a drawing of  $G'$ , but instead of using the bisection of the intersection of a primal and a dual circle, we use a circular arc with a different angle; see Fig. 18a. Let  $e = (u, v)$  be an edge of  $G'$  directed from  $u$  to  $v$ , and let  $l(e)$  be the lens region of  $e$  between the primal-dual circles  $d(e)$  and  $d'(e)$ . W.l.o.g., assume that the  $90^\circ$  angle inside  $l(e)$  is between  $d'(e)$  and  $d(e)$  in counter-clockwise order around  $u$ . In the proof of Theorem 2, we would draw  $e$  as a bisection of  $l(e)$ . We draw  $e$  that the angle between  $d'(e)$  and  $(u, v)$  at  $u$  is  $45^\circ + \varepsilon/2$  and the angle between  $e$  and  $d(e)$  at  $u$  is  $45^\circ - \varepsilon/2$ .

Informally, this means that all outgoing edges at a vertex are “rotated” by  $\varepsilon/2$  in counter-clockwise direction, and all incoming edges at a vertex are “rotated” by  $\varepsilon/2$  in clockwise direction compared to a plane circular-arc drawing of  $G'$ .



(a) Drawing a directed edge  $e = (u, v)$  (b) Eliminating a vertex  $v$  and adding the edge  $(u, w)$  inside the circle  $d(e_1)$

Fig. 18: Illustrations for the proof of Lemma 5.

Since opposite edges of a vertex  $u$  have the same direction with respect to  $u$ , they are rotated by the same angle, so they are still tangent. Further, since adjacent edges at  $u$  have a different direction with respect to  $u$ , the angle between them is now either  $90^\circ + \varepsilon$  or  $90^\circ - \varepsilon$ .

5 We then use the same procedure as in Theorem 2 to eliminate vertices from  $G'$  and obtain a plane  $\varepsilon$ -regular Lombardi drawing of  $G$ . In every step of this procedure, we eliminate a vertex  $v$  from  $G'$  and add an edge between two pairs of its adjacent vertices (without introducing self-loops); see Fig. 18b. Let  $u$  and  $w$  be two neighbors of  $v$  in  $G'$  such that we want to obtain the edge  $e = (u, w)$  in  $G$ . W.l.o.g., assume that the edge  $e_1 = (u, v)$  is directed from  $u$  to  $v$  in  $G'$  and  
 10 in  $G$ . W.l.o.g., assume that the edge  $e_2 = (v, w)$  is directed from  $v$  to  $w$  in  $G'$  and that the edge  $e_2 = (v, w)$  is directed from  $v$  to  $w$  in  $G'$ . Following the proof of Theorem 2,  $e_1$  lies in the lens region  $l(e_1)$  between disks  $d(e_1)$  and  $d'(e_1)$ , and  $e_2$  lies in the lens region  $l(e_2)$  between disks  $d(e_2) = d(e_1)$  and  $d'(e_2)$ . Hence,  $u$  and  $w$  lie on a common circle  $d(e_1)$  of the primal-dual circle packing. Assume  
 15 that the  $90^\circ$  angle inside  $l(e_1)$  is between  $d'(e_1)$  and  $d(e_1)$  in counter-clockwise order around  $u$ ; the other case is symmetric. By the direction of the edges  $e_1$  and  $e_2$ , the angle between  $e_1$  and  $d(e_1)$  is  $45^\circ - \varepsilon/2$  in counter-clockwise around  $u$  and the angle between  $d(e_1)$  and  $e_2$  is also  $45^\circ - \varepsilon/2$  in counter-clockwise direction around  $w$ . Hence, we can draw the edge  $e$  as a circular arc inside  $d(e_1)$   
 20 with angle  $45^\circ - \varepsilon/2$  to  $d(e_1)$  at both  $u$  and  $w$ . We keep the ports at both vertices and by directing the edge from  $u$  to  $w$  we also keep a direction of the edges that satisfies the above property. Thus, we obtain a plane  $\varepsilon$ -regular Lombardi drawing of  $G$ .  $\square$

**Lemma 6.** Let  $G = (V, E)$  be a 4-regular plane multigraph with a plane  $\varepsilon$ -angle Lombardi drawing  $\Gamma$ . Then, any lens multiplication  $G'$  of  $G$  also admits a plane  
 25  $\varepsilon$ -angle Lombardi drawing.



*Proof.* Let  $f$  be a lens in  $\Gamma$  spanned by two vertices  $u$  and  $v$ . We denote the two edges bounding the lens as  $e_1$  and  $e_2$ . Let  $\alpha \in [90^\circ - \varepsilon, 90^\circ + \varepsilon]$  be the angle between  $e_1$  and  $e_2$  in both end-vertices. We define the bisecting circular arc  $b$  of  $f$  as the unique circular arc connecting  $u$  and  $v$  with an angle of  $\alpha/2$  to both  $e_1$  and  $e_2$ . See Fig. 4 for an example.

Let  $p$  be the midpoint of  $b$ . If we draw circular arcs  $a_1$  and  $a_2$  from both  $u$  to  $p$  and circular arcs  $a_3$  and  $a_4$  from  $v$  to  $p$  that have the same tangents as  $e_1$  and  $e_2$  in  $u$  and  $v$ , then these four arcs meet at  $p$  such that the angle between  $a_1$  and  $a_2$  as well as the angle between  $a_3$  and  $a_4$  is  $\alpha$ , whereas the angle between  $a_1$  and  $a_4$  and the angle between  $a_2$  and  $a_3$  is  $180^\circ - \alpha \in [90^\circ - \varepsilon, 90^\circ + \varepsilon]$ . Further, each such arc lies inside lens  $f$  and hence does not cross any other arc of  $\Gamma$ . The resulting drawing is thus a plane  $\varepsilon$ -angle Lombardi drawing of a 4-regular multigraph that is derived from  $G$  by subdividing the lens  $f$  with a new degree-4 vertex.

By repeating this construction inside the new lenses we can create plane  $\varepsilon$ -angle Lombardi drawings that replace lenses by chains of smaller lenses. .  $\square$

**Lemma 8.** *Let  $G = (V, E)$  be a 4-regular plane multigraph with a plane  $\varepsilon$ -angle Lombardi drawing  $\Gamma$ . Then, any lens extension of  $G$  admits a plane  $(\varepsilon + \varepsilon')$ -angle Lombardi drawing for every  $\varepsilon' > 0$ .*

*Proof.* Let  $x \in V$  be the vertex that we want to perform the lens extension on such that we get the edges  $(u, a), (u, b), (v, c), (v, d)$  in the obtained graph  $G'$ . Let  $\alpha$  be the angle between the tangents of  $(x, a)$  and  $(x, b)$  at  $x$  in  $\Gamma$ . Since  $\Gamma$  is a plane  $\varepsilon$ -angle Lombardi drawing, we have that  $\alpha \leq 90^\circ + \varepsilon$ . Further, the angle between the tangents of  $(x, c)$  and  $(x, d)$  at  $x$  in  $\Gamma$  is also  $\alpha$ , while the angles between the tangents of  $(x, b)$  and  $(x, c)$  at  $x$  and between the tangents of  $(x, d)$  and  $(x, a)$  at  $x$  are both  $180^\circ - \alpha$ . We apply the Möbius-transformation on  $\Gamma$  that maps the edges  $(x, a)$  and  $(x, d)$  to straight-line segments and  $a$  lies on the same  $y$ -coordinate and to the right of  $x$ ; hence,  $d$  lies strictly below  $x$ .

We aim to place  $v$  such that the angle between the arcs  $(v, c)$  and  $(v, d)$  is  $\alpha + \lambda$  for some  $0 < \lambda \leq \varepsilon'$  which we will show how to choose later. We have fixed ports at  $c$  and  $d$  and a fixed angle  $\alpha + \lambda$  at  $v$ . According to Property 1, all possible positions of  $v$  lie on a circle through  $c$  and  $d$ . Note that the circle through  $c, d, x$  describes all possible positions of neighbors of  $c$  and  $d$  with angle  $\alpha$ . Since the desired angle gets larger, the position circle for  $v$  contains a point  $v_d$  on the straight-line edge  $(x, d)$  and a point  $v_c$  on the half-line starting from  $x$  with the angle of the port used by the arc  $(x, c)$ ; see Fig. 19a. We denote by  $C_v^\lambda$  the circular arc between  $v_c$  and  $v_d$  on the placement circle of  $v$  that gives the angle  $\alpha + \lambda$  at  $v$ . We do the same construction for  $u$  to obtain the circular arc  $C_u^\lambda$  between  $u_a$  and  $u_b$ .

Since the drawing of  $G$  is plane, there is some non-empty region in which we can move  $x$  such that the arcs  $(x, a), (x, b), (x, c), (x, d)$  are drawn with the same ports at  $a, b, c, d$  and do not cross any other edge of the drawing. We choose  $\lambda$  as the largest value with  $0 < \lambda \leq \varepsilon'$  such that the two circular arcs  $C_u$  and  $C_v$  lie completely inside this region.

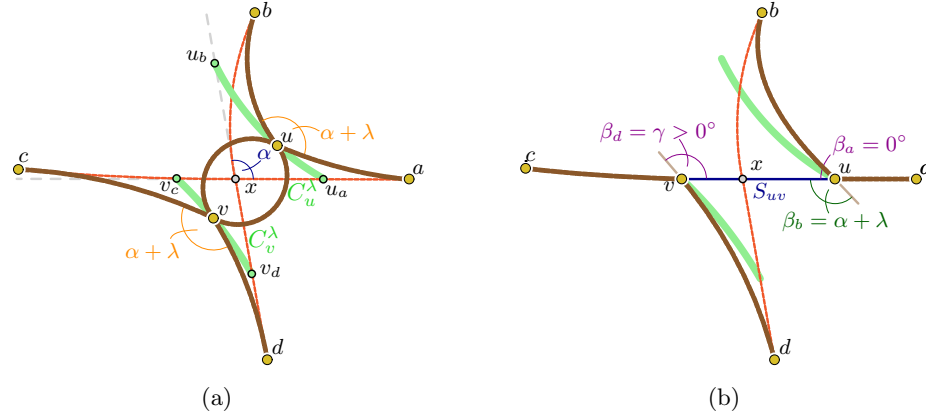


Fig. 19: (a) The circular arc  $C_u^\lambda$  between  $u_a$  and  $u_b$  on the placement circles of  $u$  and the circular arc  $C_v^\lambda$  between  $v_c$  and  $v_d$  on the placement circles of  $v$ . (b) Placing  $u$  on  $u_a$  and  $v$  on  $v_c$  gives  $\beta_a = 0^\circ$ .

We now have to find a pair of points on  $C_v^\lambda$  and  $C_u^\lambda$  such that we can connect them via a lens. The ports of the two arcs we seek to draw between  $u$  and  $v$  lie opposite of the ports used by the arcs  $(u, a)$ ,  $(u, b)$ ,  $(v, c)$ , and  $(v, d)$ . We label the ports at  $u$  and  $v$  as  $p_u^a$  opposite of  $(u, a)$  at  $u$ , as  $p_u^b$  opposite of  $(u, b)$  at  $u$ , as  $p_v^c$  opposite of  $(v, c)$  at  $v$ , and as  $p_v^d$  opposite of  $(v, d)$  at  $v$ . We have to find a pair of points on  $C_u^\lambda$  and  $C_v^\lambda$  such that these ports are “compatible”: Take a point  $q_u$  on  $C_u^\lambda$  and a point  $q_v$  on  $C_v^\lambda$  and connect them by a segment  $S_{uv}$ . Then the angle  $\beta_b$  between  $S_{uv}$  and  $p_u^b$  has to be the same as the angle  $\beta_c$  between  $S_{uv}$  and  $p_v^c$ , and the angle  $\beta_a$  between  $S_{uv}$  and  $p_u^a$  has to be the same as the angle  $\beta_d$  between  $S_{uv}$  and  $p_v^d$ . By construction, we have that  $\beta_a + \beta_b = 90^\circ + \alpha + \lambda$  and  $\beta_c + \beta_d = 90^\circ + \alpha + \lambda$ , so it suffices to find a pair of points such that  $\beta_a = \beta_d$ .

Assume that  $v$  is placed on  $v_c$  and  $u$  is placed on  $u_a$ ; see Fig. 19b. The edge  $(x, a)$  is drawn as a straight-line segment, and the edge  $(x, c)$  uses the port opposite of the one of  $(x, a)$ . Hence, the segment  $S_{uv}$  is a segment through  $x$ . Furthermore, it uses exactly the port  $p_u^a$  at  $u$ , so we have  $\beta_a = 0^\circ$ . On the other hand,  $\beta_d$  is strictly positive: The segment  $(x, d)$  enters  $x$  with an angle of  $\gamma = 180^\circ - \alpha > 0^\circ$  to the segment  $(x, v)$ . Since  $v$  lies to the left of  $x$ , the angle described between the tangent of the circular arc  $(v, d)$  at  $v$  and the segment  $(v, x)$  is strictly larger than  $\gamma$ . Since  $\beta_d$  is described by the same tangent and segment, we have that  $\beta_d = \gamma > 0^\circ$ .

Now assume that  $v$  is placed on  $v_d$  and  $u$  is placed on  $u_b$ ; see Fig. 20a. The edge  $(x, d)$  is drawn as a straight-line segment, and the edge  $(x, b)$  uses the port opposite of the one of  $(x, d)$ . Hence, the segment  $S_{uv}$  is a segment through  $x$ . Furthermore, it uses exactly the port  $p_u^d$  at  $u$ , so we have  $\beta_d = 0^\circ$ . On the other hand,  $\beta_a$  is strictly positive: The segment  $(x, a)$  enters  $x$  with an angle of  $\delta = 90^\circ + \alpha > 0^\circ$  to the segment  $(x, v)$ . Since  $u$  lies above  $x$ , the angle described between the tangent of the circular arc  $(u, a)$  at  $u$  and the

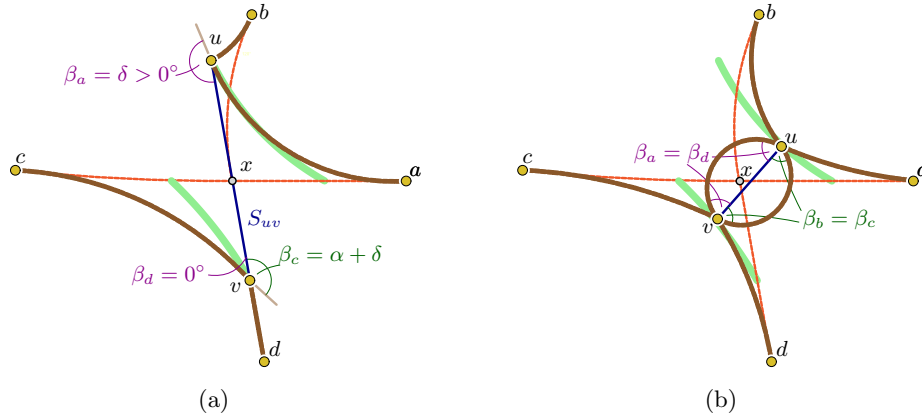


Fig. 20: (a) Placing  $u$  on  $u_b$  and  $v$  on  $v_d$  gives  $\beta_d = 0^\circ$ . (b) Placing  $u$  and  $v$  such that  $\beta_a = \beta_d$  gives a lens between  $u$  and  $v$  with the desired angles.

segment  $(u, x)$  is strictly larger than  $\delta$ . Since  $\beta_d$  is described by the same tangent and segment, we have that  $\beta_d = \delta > 0^\circ$ .

Hence, we have found a pair of points for  $u$  and  $v$  such that  $\beta_a = 0^\circ$  and  $\beta_d = \gamma > 0^\circ$  and we have found a pair of points for  $u$  and  $v$  such that  $\beta_a = \delta > 0^\circ$  and  $\beta_d = 0^\circ$ . Since we can move  $u$  and  $v$  freely along the curves  $C_u$  and  $C_v$  between these pairs of points,  $\beta_a$  can become any angle between  $0^\circ$  and  $\delta$  and  $\beta_d$  can become any angle between  $0^\circ$  and  $\gamma$ . Thus, there has to exist some pair of points for  $u$  and  $v$  such that  $\beta_a = \beta_d$ ; see Fig. 20b. We choose this pair of points and connect  $u$  and  $v$  by two circular arcs such that one of them uses the ports  $p_u^a$  and  $p_v^d$  and the other one uses the ports  $p_u^b$  and  $p_v^c$ . Note that the arcs  $(u, a)$  and  $(u, b)$  are now drawn the same way as if we moved  $x$  onto the determined position of  $u$  and the arcs  $(v, c)$  and  $(v, d)$  are now drawn the same way as if we moved  $x$  onto the determined position of  $v$ . Hence, by the choice of  $\lambda$ , they do not introduce any crossing and thus the drawing is plane.  $\square$

**Theorem 7.** Let  $G = (V, E)$  be a biconnected 4-regular plane multigraph and let  $\varepsilon > 0$ . Then  $G$  admits a plane  $\varepsilon$ -angle Lombardi drawing.

*Proof.* If  $G$  has at most 3 vertices, then we obtain a plane Lombardi drawing of  $G$  by Lemma 9. So assume that  $G$  is a biconnected 4-regular plane graph with  $n \geq 4$ . We seek to draw  $G$  by recursively by splitting it into smaller graphs. We prove our algorithm by induction on the number of vertices; to this end, suppose that every biconnected 4-regular plane graph with at most  $n - 1$  vertices admits a plane  $\varepsilon'$ -angle Lombardi drawing for every  $\varepsilon' > 0$ ; this holds initially for  $n = 4$ . We proceed as follows.

**Case 1.**  $G$  is polyhedral. In this case, we can draw it plane Lombardi using Theorem 2.

**Case 2.**  $G$  contains a *multilens*, that is, a sequence of lenses between the vertices  $u_1, \dots, u_k$  with  $k \geq 2$ . We contract the lenses to a single lens, that is, we

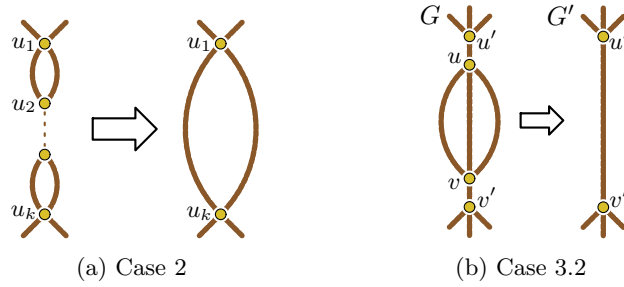


Fig. 21: Illustrations for the proof of Theorem 7.

remove the vertices  $u_2, \dots, u_{k-1}$  and their incident edges from  $G$  and add two edges between  $u_1$  and  $u_k$  to form a new graph  $G'$ ; see Fig. 21a. This operation is essentially a reverse lens multiplication and introduces no self-loops. It also preserves biconnectivity since  $u_1$  and  $u_k$  form a separation pair in  $G$ , so any cutvertex in  $G'$  would also be a cutvertex in  $G$ . Hence,  $G'$  is a biconnected 4-regular plane graph with  $n - k + 1 \leq n - 1$  vertices and by induction admits a plane  $\varepsilon$ -angle Lombardi drawing. Furthermore,  $G$  is a lens multiplication of  $G'$  on the lens  $(u_1, u_k)$ , so we can use Lemma 6 to obtain a plane  $\varepsilon$ -angle Lombardi drawing of  $G$ .

**Case 3.**  $G$  contains a lens between two vertices  $u$  and  $v$ , but it contains no multilens. We consider three subcases based on the number of edges between  $u$  and  $v$  in  $G$ .

**Case 3.1.** There are four edges between  $u$  and  $v$  in  $G$ . Since  $G$  is 4-regular, it consists exactly of these two vertices and four edges and can be drawn by Lemma 9.

**Case 3.2.** There are three edges between  $u$  and  $v$  in  $G$ ; see Fig. 21b. Then there exists also some edge  $(u, u')$  and some edge  $(v, v')$  in  $G$ . Since  $G$  is biconnected, we have  $u' \neq v'$ ; otherwise, it would be a cutvertex. We remove  $u$  and  $v$  from  $G$  and add an edge between  $u'$  and  $v'$  to form a new graph  $G'$ . This operation preserves biconnectivity as  $u'$  and  $v'$  form a separation pair in  $G$  and it introduces no self-loops because  $v \neq v'$ . Hence, the graph  $G'$  is a biconnected 4-regular plane graph with  $n - 2$  vertices and by induction admits a plane  $\varepsilon$ -angle Lombardi drawing. Let  $G''$  be the graph that consists of  $u$  and  $v$  and four multi-edges between them. This graph has a plane  $\varepsilon$ -regular Lombardi drawing by Lemma 9. Furthermore,  $G$  can be obtained by adding  $G'$  and  $G''$  along the edge  $(u', v')$  of  $G'$  and one of the edges of  $G''$ . Using Lemma 7, we can obtain a plane  $\varepsilon$ -angle Lombardi drawing of  $G$ .

**Case 3.3.** There are two edges between  $u$  and  $v$  in  $G$ . We consider two subcases.

**Case 3.3.1.** Removal of  $u$  and  $v$  from  $G$  preserves connectivity; see Fig. 22a. We contract  $u$  and  $v$  to a new vertex: we remove them from  $G$  and add a new vertex  $x$  that is connected to the neighbors of  $u$  and  $v$  different from  $u$  and  $v$  to form  $G'$ . This operation preserves biconnectivity: Since  $G$  is biconnected, the only cutvertex in  $G'$  can be  $x$ ; but since the removal of  $u$  and  $v$  from  $G$  preserves

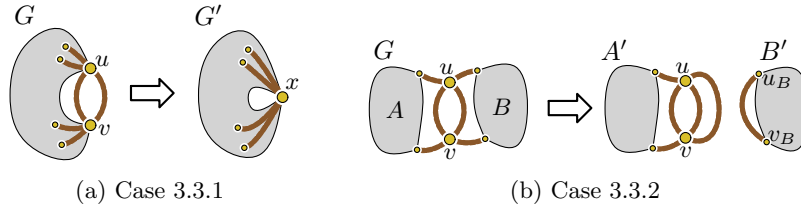


Fig. 22: Illustrations for Case 3.3 in the proof of Theorem 7.

connectivity, so does the merged vertex  $x$ . Since there are exactly two edges between  $u$  and  $v$ , the new vertex  $x$  has degree 4. Hence,  $G'$  is a biconnected 4-regular plane graph with  $n-1$  vertices and by induction admits a plane  $\varepsilon/2$ -angle Lombardi drawing. Furthermore,  $G$  can be obtained from  $G'$  by a lens extension on  $x$ . We obtain a plane  $\varepsilon$ -angle Lombardi drawing of  $G$  using Lemma 8.

**Case 3.3.2.** The removal of  $u$  and  $v$  from  $G$  disconnects the graph, that is,  $u$  and  $v$  form a separation pair in  $G$ ; see Fig. 22b. Since there are exactly two edges between  $u$  and  $v$ , their removal disconnects  $G$  into two connected components  $A$  and  $B$  with at least two vertices each (otherwise, there would be a self-loop). Furthermore,  $G$  contains an edge from  $u$  to a vertex  $u_A$  in  $A$  and another edge from  $u$  to a vertex  $u_B$  in  $B$ . If this would not be the case than  $v$  would be a cutvertex in  $G$ . Analogously, there is an edge from  $v$  to a vertex  $v_A$  in  $A$  and an edge from  $v$  to a vertex  $v_B$  in  $B$ . We have  $u_A \neq v_A$  (and  $u_B \neq v_B$ ); otherwise, this vertex would be a cutvertex in  $G$ .

Let  $A'$  be the graph  $G-B$  with an additional edge between  $u$  and  $v$ . Since  $G$  is biconnected, there are two disjoint paths in  $G$  between any two vertices from  $A$ . Only one of these paths can “leave”  $A$  through the separation pair  $u, v$ . Hence, we can redirect the part outside  $A$  to the new edge  $(u, v)$  in  $A'$ , which shows that every two vertices in  $A'$  are connected with at least two disjoint paths. This shows that  $A'$  is biconnected.

Let  $B'$  be the graph  $B$  with an additional edge between  $u_B$  and  $v_B$ . We can show that  $B'$  is biconnected by the same arguments we have applied for  $A'$ : In  $G$  there have to be two disjoint paths between every vertex pair from  $B$ . Only one of these paths can leave  $B$  over the separation pair  $u, v$  and this part can be replaced by the new edge that we added to  $B'$ . Hence between every two vertices in  $B'$  we have two disjoint paths, which proves that  $B'$  is a biconnected 4-regular plane graph with at most  $n-4$  vertices. By induction  $B'$  admits a plane  $\varepsilon$ -angle Lombardi drawing. Furthermore,  $G$  can be obtained by adding  $A'$  and  $B'$  along one of the edges between  $u$  and  $v$  of  $A'$  and the edge  $(u_B, v_B)$  of  $B'$ . Using Lemma 7, we can obtain a plane  $\varepsilon$ -angle Lombardi drawing of  $G$ .

**Case 4.**  $G$  is simple, but not 3-connected, so there exists at least one separation pair that splits  $G$  into at least two connected components. Let  $A_{u,v}$  be a smallest connected component induced by the separation pair  $u, v$ . We say that  $u, v$  is a *minimal separation pair* if  $A_{u,v}$  does not contain any separation pair and there is no separation pair between a vertex of  $A_{u,v}$  and either  $u$  or  $v$ .

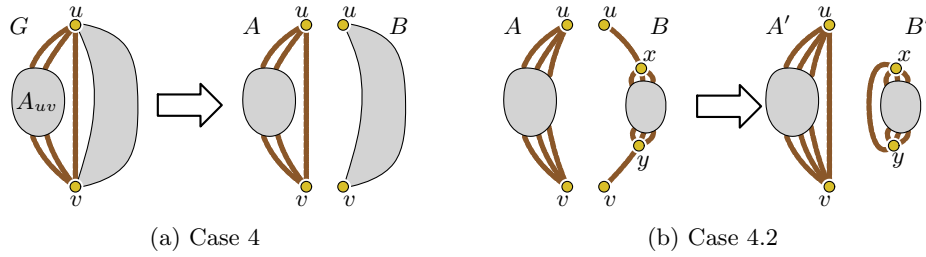


Fig. 23: Illustrations for Case 4 in the proof of Theorem 7.

We create two biconnected 4-regular plane graphs as follows; see Fig. 23a. Let  $A$  be the subgraph of  $G$  induced by the vertices in  $A_{u,v}$ ,  $u$ , and  $v$ , let  $B$  be the subgraph of  $G$  that contains all vertices not in  $A_{u,v}$  and all edges not in  $A$ ; in particular, there is no edge  $(u, v)$  in  $B$ . By this construction, all edges of  $G$  are either part of  $A$  or part of  $B$  and both  $A$  and  $B$  are connected, and every vertex is part of either  $A$  or  $B$ , except the two vertices  $u$  and  $v$  which are part of both. However,  $A$  and  $B$  are not 4-regular, so we create two 4-regular graphs  $A'$  and  $B'$  for the recursion as follows. Let  $\deg_A(u)$ ,  $\deg_A(v)$ ,  $\deg_B(u)$ ,  $\deg_B(v)$  be the degree of  $u$  and  $v$  in  $A$  and  $B$ , respectively, with  $\deg_A(u) + \deg_B(u) = \deg_A(v) + \deg_B(v) = 4$ .

**Case 4.1.**  $\deg_A(u) = 1$  or  $\deg_A(v) = 1$ . W.l.o.g., let  $\deg_A(u) = 1$ . Let  $x$  be the neighbor of  $u$  in  $A$ . We have that  $x \neq v$  since otherwise  $A$  consists only of a single edge (if  $\deg_A(v) = 1$ ) or  $v$  is a cutvertex in  $G$  (if  $\deg_A(v) = 3$ ). Then  $x, v$  is a separation pair of  $G$  whose removal gives a connected component  $A_{x,v}$  with less vertices than  $A_{u,v}$ , as it contains the same vertices but not  $x$ , contradicting the minimality of the separation pair  $u, v$ .

**Case 4.2.**  $\deg_A(u) = \deg_A(v) = 3$ ; see Fig. 23b. We add an edge between  $u$  and  $v$  to  $A$  to obtain the graph  $A'$ . The resulting graph is biconnected: consider any pair of vertices  $a, b \in A'$ . There were at least two vertex-disjoint paths in  $G$  between  $a$  and  $b$ . Since  $u, v$  is a separation pair in  $G$ , at most one of these two paths traverses vertices in  $G - A$ , and any path through these vertices must contain  $u$  and  $v$ . Hence, there is a path that traverses the same edges in  $A'$  and uses the newly introduced edge between  $u$  and  $v$  instead.

We remove  $u$  and  $v$  from  $B$  and add an edge between their neighbors to form  $B'$ . Let  $x$  be the neighbor of  $u$  in  $B$  and let  $y$  be the neighbor of  $v$  in  $B$ . We have that  $x \neq y$  since otherwise  $x$  would be a cutvertex in  $G$ . Hence, we introduce no self-loops. With a similar argument,  $B'$  is also biconnected, as any path between two vertices through vertices in  $A$  has to traverse  $u$  and  $v$  and—since they both have degree 1 in  $B$ —their neighbors, so the path can use the newly introduced edge instead.

We recursively obtain a plane  $\varepsilon$ -angle Lombardi drawing of  $A'$  and  $B'$ . Since both  $A'$  and  $B'$  have fewer vertices than  $G$ , they admit one by induction. To obtain a drawing of  $G$  from  $A'$  and  $B'$ , we have to remove the edge  $(u, v)$  from  $A'$  and the edge  $(x, y)$  from  $B'$  and we have to add the edges  $(u, x)$  and  $(v, y)$ . This

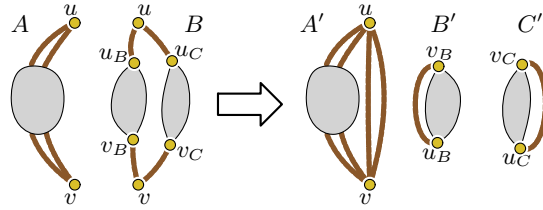


Fig. 24: Illustration for Case 4.3.1 in the proof of Theorem 7.

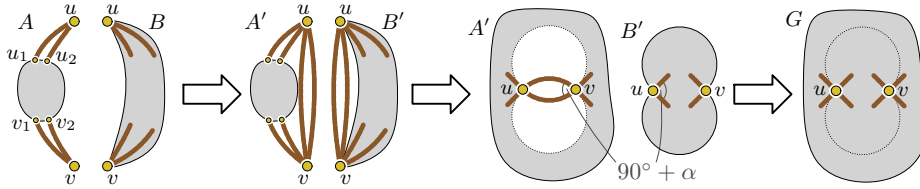


Fig. 25: Illustration for Case 4.3.2 in the proof of Theorem 7.

procedure is equivalent to adding  $A'$  and  $B'$  along these respective edges, so we can solve it using the algorithm described in Lemma 7.

**Case 4.3.**  $\deg_A(u) = \deg_A(v) = 2$ . We consider two more subcases.

**Case 4.3.1.** The separation pair  $u, v$  splits  $G$  into three connected components  $A_{u,v}$ ,  $B_{u,v}$ , and  $C_{u,v}$ ; see Fig. 24. We add two edges between  $u$  and  $v$  to  $A$  to obtain  $A'$ . Let  $u_B$  be the neighbor of  $u$  in  $B_{u,v}$  and let  $v_B$  be the neighbor of  $v$  in  $B_{u,v}$ . We have that  $u_B \neq v_B$ , as otherwise it would be a cutvertex of  $G$ . We obtain the 4-regular multigraph  $B'$  by adding an edge between  $u_B$  and  $v_B$  to  $B_{u,v}$ . By the same argument as in Case 3.3.2,  $B'$  is biconnected. Analogously, we obtain the biconnected 4-regular multigraph  $C'$  by adding an edge between the neighbor  $u_C$  of  $u$  in  $C_{u,v}$  and the neighbor  $v_C$  of  $v$  in  $C_{u,v}$  to  $C_{u,v}$ . We recursively create a plane  $\varepsilon$ -angle Lombardi drawing of  $A'$ ,  $B'$ , and  $C'$ . Then, we create a plane  $\varepsilon$ -angle Lombardi drawing with the use of Lemma 7 by adding  $A'$  and  $B$  along one edge between  $u$  and  $v$  of  $A'$  and the edge  $(u_B, v_B)$  of  $B$ , and adding the resulting graph and  $C$  along the other edge between  $u$  and  $v$  and the edge  $(u_C, v_C)$  of  $C$ .

**Case 4.3.2.** The separation pair  $u, v$  splits  $G$  into two connected components  $A_{u,v}$  and  $B_{u,v}$ ; see Fig. 25. In this case, the graph  $B$  consists of  $B_{u,v}$ ,  $u$ , and  $v$  and the edges incident to  $u$  or  $v$  and a vertex of  $B_{u,v}$ .

We add two edges between  $u$  and  $v$  to both graphs  $A$  and  $B$  to obtain  $A'$  and  $B'$ . Let  $M$  and  $M'$  be the primal-dual pair for which  $A'$  is the medial graph. We claim that  $M$  or  $M'$  is simple. Let  $u_1$  and  $u_2$  be the neighbors of  $u$  in  $A$  and let  $v_1$  and  $v_2$  be the neighbors of  $v$  in  $A$ . Since  $G$  is simple, there is no multi-edge between  $u$  and  $v$  in  $A$ . Furthermore, there is no single edge  $(u, v)$  in  $A$ , since otherwise  $u$  and  $v$  would each only have one neighbor in  $A_{u,v}$  and these neighbors would be a separation pair of  $G$  that induces a smaller connected component. Thus, each of  $u_1, u_2, v_1, v_2$  is different from  $u$  and  $v$  and we

introduce no self-loops. By construction, the graph  $A_{u,v}$  contains no separation pair and thus has either at most 3 vertices or is 3-connected. We claim that  $A'$  is 3-connected. If  $A_{u,v}$  has only 1 vertex, then  $u_1 = u_2$ , so there is a multi-edge in  $A_{u,v}$  which contradicts simplicity of  $G$ . If  $A_{u,v}$  has only 2 vertices, then there has to be a multi-edge between them, which again contradicts simplicity of  $G$ . If  $A_{u,v}$  has only 3 vertices, then there have to be 4 edges in  $A_{u,v}$ , which also contradicts simplicity of  $G$ . If  $A_{u,v}$  has at least 4 vertices, then  $u$  and  $v$  have at least 3 different neighbors in  $A_{u,v}$ , as otherwise there would be a cutvertex or a separation pair that gives a smaller connected component than the separation pair  $u, v$ . Thus, if  $u$  and  $v$  are connected to at least 3 vertices of  $A_{u,v}$  and  $u$  and  $v$  are connected by an edge, which preserves 3-connectivity. Hence,  $A'$  is 3-connected. Since  $G$  is simple, there is no multi-edge between  $u$  and  $v$  in  $A$ . Furthermore, there is no single edge  $(u, v)$  in  $A$ , since otherwise  $u$  and  $v$  would each only have one neighbor in  $A_{u,v}$  and these neighbors would be a separation pair of  $G$  that induces a smaller connected component. Hence,  $A'$  has no separation pair and exactly one multi-edge between  $u$  and  $v$ . By Lemma 2, that means that  $M$  and  $M'$  have exactly one pair of parallel edges in total, so one of them has to be simple.

We recursively obtain a plane  $\varepsilon$ -angle Lombardi drawing of  $B'$ . Let  $90^\circ + \alpha$  be the angle described by the tangents of the two edges between  $u$  and  $v$  at  $u$ . Note that  $\alpha$  might be negative, but  $|\alpha| \leq \varepsilon$ . Since the primal or dual of  $A'$  is simple, we obtain a plane  $|\alpha|$ -regular Lombardi drawing of  $A'$  by Lemma 5. Thus, the angle described by the tangents of the two edges between  $u$  and  $v$  at  $u$  is either  $90^\circ + \alpha$  or  $90^\circ - \alpha$ . We can make sure that the angle is  $90^\circ + \alpha$  by inverting the direction of all edges in the proof of Lemma 5 in case it is not.

We perform a Möbius-transformation on the drawing of  $A'$  such that the edges between  $u$  and  $v$  are drawn with an angle of  $45^\circ + \alpha/2$  between either edge and the segment between  $u$  and  $v$ . We pick the Möbius-transformation such that  $u$  and  $v$  are very close to each other; in particular, we want them to be close enough such that the two circles that the edges between  $u$  and  $v$  lie on contain no other vertex of  $A'$  and no edges of  $A'$  that is incident to neither  $u$  nor  $v$ . Note that the radius of these circles are the same and approach 0 as the distance between  $u$  and  $v$  approaches 0; hence, such a Möbius-transformation exists.

We apply another Möbius-transformation on  $B'$  such that the distance between  $u$  and  $v$  is the same as in the drawing of  $A'$  and such that the two edges between  $u$  and  $v$  are drawn with an angle of  $135^\circ - \alpha/2$  between either edge and the segment between  $u$  and  $v$ . We now place the drawing of  $B'$  on the drawing of  $A'$  such that both copies of  $u$  lie on the same coordinate and both copies of  $v$  lie on the same coordinate and then we remove all edges between  $u$  and  $v$ . By construction, the whole drawing of  $B'$  lies inside the region described by the two edges between  $u$  and  $v$  in the drawing of  $B'$ . Further, since these edges lie on the same circles as the two edges between  $u$  and  $v$  in  $A'$ , this region contains no vertices or edges in the drawing of  $A'$  (except  $u$  and  $v$  and their incident edges themselves). Since the drawings of  $A'$  and  $B'$  are plane and we cannot introduce



a crossing between an edge of  $A'$  and an edge of  $B'$  after removing the multi-edges between  $u$  and  $v$ , the resulting drawing of  $G$  is also plane. Since  $u$  and  $v$  use the same ports in the drawing of  $A'$  and the drawing of  $B'$ , the resulting drawing is a plane  $|\alpha|$ -angle Lombardi drawing of  $G$ . Because of  $|\alpha| \leq \varepsilon$ , this  
5 drawing is also a plane  $\varepsilon$ -angle Lombardi drawing of  $G$ .  $\square$